Materials and methods

Patient and Specimens

We used 314 pairs of HCC tissues (pairs refer to tumor tissue and adjacent tissue form the same patients) from patients who underwent liver biopsy at the Hepatic Surgery Center of Tongji Hospital of University of Science and Technology (HUST, Wuhan, China) between February 2015 and March 2018. All samples were pathologically diagnosed with HCC and followed up for prognostic assessment. All samples were used for Sequencing of the CTNNB1 exons 3. 196 pairs of HCC tissues form this cohort were utilized to construct microarrays for immunohistochemistry (IHC) experiments. 99 pairs of HCC tissues form this cohort were used for the Quantitative real time polymerase chain reaction (q-PCR). All patients provided signed informed consent forms. The study was approved by the Ethics Committee of Tongji Hospital (HUST, Wuhan, China), and sample tissues were utilized in accordance with the appropriate regulations.

Cell Lines and Cell Culture

HEK 293T cell line and Hepa1-6 cell line were purchased from China Center for Type Culture Collection (CCTCC, Wuhan, China). HEK 293T and Hepa1-6 cells were cultured in Dulbecco's modified Eagle's medium (DMEM, HyClone, #SH30022.01) containing 10% FBS (Gibco, #10099) at 37℃ and 5% CO_2 in an incubator. Both of the cell lines were routinely authenticated and were free of *Mycoplasma* contamination. $CD8^+$ T cells were cultured in RPMI 1640 medium (HyClone; #SH30809.01) supplemented with 10% FBS (Gibco, #10099), 1% penicillin/streptomycin (Kerui; #KR151400), 5μg/mL CD3ε (Biolend; #100340), 1μg/mL CD28 (Biolend; #302934) and 20 ng/mL mIL2 (R&D Systems; #402-ML) at 37°C and 5% CO_2.

Animal Studies

All animal care and experimental protocols were performed according to the National Institutes of Health Guidelines for the Care and Use of Laboratory Animals and approved by the Ethics Committee of Tongji Hospital (HUST, Wuhan, China). $MMP9^{F/F}$ and $MMP9^{\Delta hep}$ mice were purchased from Cyagen Biosciences Inc. For HCC induced by hydrodynamic tail vein injection (HTVi), 6-week-old male C57BL/6J mice (Gempharmatech Co., Ltd) (n = 6) were used. For each mouse, *pT3-ΔN90-CTNNB1* (10μg)/*pT3-vector* (10μg)/*pT3-EF1aH-myr-AKT* (20μg)/*pT3-EF1aH-c-Met* (20μg)/*pT3-EF1a-MYC-IRES-Luciferase* (15μg)/*SB100* transposase-encoding plasmid (1/4 of the total plasmid mass) were dissolved in 2 mL 0.9% Nacl solution and injected 10% of the weight of each mouse in volume in 5-8 seconds. Equivalent DNA concentration between different batches of DNA was confirmed to ensure reproducibility among experiments. Mice were monitored and euthanized when they developed large abdominal masses and become moribund. At the end of the experiment, solid tumors were collected and analyzed by IHC, flow cytometry and/or mIF.

In the subcutaneous tumor formation assay, 2×10^6 logarithmic growth-phase Hepa1-6 cells in 100μL of DMEM (HyClone, #SH30022.01) were injected into the axillary regions of 4-week-old BALB/C male nude mice (n = 7) and 6-week-old male C57BL/6J mice (Gempharmatech Co., Ltd) (n = 6). For orthotopic HCC models, 6-week-old male C57BL/6J mice (Gempharmatech Co., Ltd) (n = 6-15) were injected in the largest liver lobe with 8×10^6 Hepa1-6 cells in 30μL of DMEM (HyClone, #SH30022.01). After 3 weeks, all the mice were sacrificed. Livers were harvested to assess the tumor burden. At the end of the experiment, solid tumors were collected and analyzed by IHC, flow cytometry and/or mIF.

For the T cell depletion experiments, mice were injected intraperitoneally with anti-CD8 (200μg, clone 53-6.7, BioXcell), anti-CD4 (200μg, clone GK1.5, Sellect), IgG2a (200μg, clone 2A3, BioXcell) or IgG2b (200μg, clone LTF-2, Sellect) twice a week. For the Macrophage depletion experiments, mice were injected intraperitoneally with Clophosome (1.4mg first day, 0.7mg every 6 days, FormuMax, #F70101C-N). For the experiments with amti-PD-1 mAbs, mice were intravenously injected with anti-PD-1 (200μg, Junmeng Jiangsu, #GC42) every three days via the tail vein. For blocking the function of MMP9, mice were injected intraperitoneally with MMP9-in-1 (20mg/kg, MedChemExpress) every two days.

All experiments were randomized according to numbers. The personnel who treated the mice were aware of the group allocation at the different stages of the experiment.

Flow Cytometry Sample Preparation and Cytokine/Surface Staining

Fresh harvest tumors were cut into small pieces (~1 mm^3) with scissors and digested with collagenase IV (1mg/mL in 10% FBS DMEM, Biosharp, #BS165) and DNaseI (0.1mg/mL in 10% FBS DMEM, Biosharp, #BS137) for 30 minutes at 37℃. Dissociated tumor samples were homogenized and filtered through a 200-mesh screen and then filtered through a 70-μm strainer. ACK Lysis Buffer (Servicebio, #G2015) was utilized to lyse erythrocytes. Single cells were resuspended in 100μL pre-cooled living cells staining mix (0.5μL/sample FVS in PBS) and incubated for 10 minutes on ice. Then cells were blocked and stained for 30 minutes with surface antibody mix (1μL/sample in PBS). For intracellular cytokine staining, cells were stimulated for 3-6 hours and treated with Phosflow Perm Buffer III (BD Pharmingen, #558050) according to the manufacturer's instructions. Finally, cells were washed, resuspended, and stored at 4℃ before acquisition on a flow cytometry instrument (CytoFLEX). Flow cytometry data were analyzed using Flowjo (BD Pharmingen, v10.3.5) software. Antibody and suppliers are listed in Supplementary Table S5.

T-Distributed Stochastic Neighbor Embedding (tSNE) analysis in FlowJo

Raw data were cleaned up to exclude doublets, debris and dead cells. In addition, cells of interest were incorporated for further analysis. Appropriate fluorescence compensated parameters were selected in each fluorescence channel. Then, the plugin "downsample" was used to down sample the events to ensure an equal number of cells per sample. All samples were concatenated together and run tSNE on this single large file for comparing multiple samples. After running tSNE, FlowJo will automatically add to separate the files using the variable "Sample ID".

Immunoblot and Coimmunoprecipitation

Suspension cells harvested by centrifugation or cultured adherent cells proteins were dispersed in RIPA Lysis Buffer (Meilunbio, #MA0151) supplemented with 1/100 Protease Inhibitor Cocktail (MedChemExpress, #HY-K0010), 1/100 Phosphatase Inhibitor Cocktail I (MedChemExpress, #HY-K0021) and 1/100 Phosphatase Inhibitor Cocktail II (MedChemExpress, #HY-Koo22) for 15 minutes on ice. For mouse tissue samples, the tissues were first homogenized using the tissue homogenizers (Servicebio, #KZ-III-F) in ice-cold above RIPA Lysis Buffer for 120 seconds (60Hz). Cell or tissue lysates were centrifuged at 12,000 rpm for 15 minutes at 4℃. Supernatants were collected and measured concentration by UV–Visible Spectrophotometer (BeckMan, #DU730). Then, the protein supernatants were adjusted to the same concentration by adding 5× SDS-PAGE

loading buffer (Servicebio, #G2075) and RIPA Lysis Buffer, and the samples were boiled at 95℃ for 10 minutes. Prepared protein samples were loaded onto 10% SDS-PAGE gels, separated by electrophoresis, and then transferred onto polyvinylidene fluoride membranes (Millipore). After transfer, membranes were blocked with TBST containing 5% skim milk for 1 hour at room temperature. After washed with TBST 3 times at room temperature (each for 5 minutes), membranes were incubated with the indicated primary antibody at 4℃ overnight. On the second day, membranes were washed with TBST 3 times (each for 10 minutes) and then incubated with secondary antibody (Horseradish Peroxidase-conjugated) for 1 hour at room temperature. Finally, membranes were washed with TBST 3 times (each for 10 minutes), and reactive bands were visualized and exposured using ECL substrate (Bio-Rad, #1705060/1705061). Antibodies and suppliers are listed in Supplementary Table S5.

For co-IP, transfected cells were lysed with IP cell lysates (Servicebio, #G2038) supplemented with 1/100 Protease Inhibitor Cocktail (MedChemExpress, #HY-K0010). Cell lysates were centrifuged at 12,000 rpm for 15 minutes at 4℃. Supernatants were incubated with co-IP-grade antibodies with rotation at 4℃ overnight. On the second day, antibodies were pull down with Protein G Magnetic Beads (MedChemExpress, #HY-K0204) with rotation for 3-4 hours at room temperature. After washing with wash buffer 6 times, samples were added 2×SDS-PAGE loading buffer (Servicebio, #G2075) and boiled at 95℃ for 10 minutes, followed by immunoblot analysis. Antibodies and suppliers are listed in Supplementary Table S5.

RT-PCR

Total RNA was extracted from cultured cells and tissues using the RNA-easy Isolation Reagent (Vazyme, #R701-01) and used as a template to generate cDNA with the HiScript III RT SuperMix for qPCR (Vazyme, #R323-01). Q-PCR was performed using the ChamQ Universal SYBR qPCR Master mix (Vazyme, #Q711-02) on a Real-Time System (Bio-Rad, #CFX Connect) and analyzed using BioRadCFX Manager (Bio-Rad, v3.0) software. Relative RNA expression levels were determined by comparative threshold cycle ($2^{-\Delta\Delta}$CT). Primers used are given in Supplementary Table S6.

Dual-luciferase reported assay

Luciferase activity was detected with the Dual Luciferase Reporter Assay Kit (Vazyme, #DL101-01) according to the manufacturer's instructions. The relative luciferase activity was determined by a GloMax 20/20 Luminometer (Promega). Luciferase activity was normalized to Renilla activity.

Immunohistochemistry and Analysis

Tissue specimens used for IHC were fixed in 4% paraformaldehyd and embedded in paraffin, and paraffin-embedded tissue sections that had been cut to 4 μm thickness. The paraffin sections were then deparaffinized, and antigen retrieval with 0.01 M sodium citrate buffer (pH6.0, Servicebio, #G1219) or Tris-EDTA buffer (pH8.0, Servicebio, #G1207), followed with 3% hydrogen peroxide incubated for 15 minutes at room temperature to block endogenous peroxidase. Next, the sections were blocked by 5% bovine serum albumin (BSA) blocking for 60 minutes at room temperature. Primary antibodies were incubated overnight at 4℃ in a humidified chamber, followed by HRP conjugated secondary antibody incubation for 45 minutes at 37℃. The binding of antibodies was detected by DAB (Servicebio, #G1212) and the reaction was stopped by immersion in distilled water

after brown color was observed under the microscope. Tissue sections were counterstained by hematoxylin (Servicebio, #G1004), dehydrated in graded ethanol, sealed with neutral balsam, photos were taken and analyzed. Antibodies and suppliers are listed in Supplementary Table S5.

Positive and negative control groups were included for each batch of immunohistochemically stained sections. The IHC staining score was calculated according to the staining intensity and the percentage of positive cells. The rules of the staining intensity scoring were as follows: 0 points (Negative); 1 points (Light brown); 2 points (Brown); 3 points (Dark brown). The rules of stained positive cells scoring were as follows: score 0 denotes less than 10%, score 1 denotes 10-25%, score 2 denotes 26-50%, score 3 denotes 51-75% and score 4 denotes more than 75% of positive stained cells. The staining intensity and extent were multiplied to generate IHC staining score. Overall scores of <6 and ≥6 were defined as low expression and high expression, respectively. IHC analyses were scored by two independent pathologists blind to the clinical data and grouping information.

Multiplex Immunofluorescence Staining

For multiplex staining, we followed the tyramide signal amplification (TSA) protocol staining method. The methods of antigen retrievaling, blocking endogenous peroxidase and BSA blocking were consistent with the IHC described above. The first primary antibody was incubated overnight at 4℃ in a humidified chamber, followed by secondary antibody incubation for 45 minutes at 37℃. Tyramide working solution was incubated for 10 minutes at room temperature and protected from light. After washing with wash buffer for 20 minutes at 42℃ and BSA blocking for 30 minutes at 37℃, the second primary antibody was incubated overnight at 4℃ in a humidified chamber. The operations were then repeated as described above until meet the desired number of primary antibodies. The sections were sealed by anti-fluorescence quenching sealed tablets (Southern Biotech, #0100-01) after cell nuclei counterstained with DAPI (Solarbio, #C0060) for 5 min. Each of the stained sections was scanned using a slide scanner (3D HISTECH, # Pannoramic SCAN II) under fluorescence conditions and analyzed using Zen Microscope (ZEISS, v2.6) software. Antibodies, suppliers and fluorescence channel are listed in Supplementary Table S5.

Plasmids and constructions

MMP9 2.0 kb promoter sequence and SBE sites truncations were cloned into the pGL4.17 vector. Mammalian expression plasmids for Flag-, HA- or Myc-tagged SIRT2, β-catenin and KDM4D and the truncated proteins were constructed by standard molecular cloning method from cDNA templates. MMP9 promoter SBE site mutation plasmid was constructed by site-directed mutagenesis. All constructs were confirmed by DNA sequencing.

Lentivirus-transduced stable cell lines

To generate stable gene over-expression or knockdown cells lines, Flag-tagged CDS of SIRT2 andSSH1 were cloned into the BamHI/SalI sites of pLenti-CMV-Puro plasmid (Addgene, #17448), or the short hairpin targeting sequences for MMP9, KDM4D and SSH1 were cloned into the pLKO.1-TRC vector (Addgene, #10879). Vectors contain Flag tag or scramble shRNA (Addgene #1864) were used as negative controls, respectively. HEK293 cells were co-transfected with pMD2.G (Addgene #12259), psPAX2 (Addgene #12260), and pLenti-CMV-Puro or pLKO.1-shRNA plasmids (ratio 1:3:4) to produce lentiviruses. Virus supernatant were collected at 48 hours post transfection, and were concentrated over 100-fold using a Lentivirus Concentration Solution

(Yeasen Biotechnology, #41101ES50), aliquots were stored at -80°C. To establish stable murine HCC cell lines, forty-eight hours post lentivirus infection, cells were selected by puromycin addition (3 μg/mL). The target sequences for specific genes were as follows are listed in Supplementary Table S6.

T cell Cytotoxicity assays

$CD8^+$ CTLs were sorted form 6-week-old male C57BL/6J mice splenocytes using a Mouse CD8+ T-Cell Isolation Kit (Sellect, #B90011) and incubated with 5μg/mL CD3ε (Biolend; #100340), 1μg/mL CD28 (Biolend; #302934) and 20 ng/mL mIL2 (R&D Systems; #402-ML) for 3 days. Prepared CTLs co-cultured with Hepa1-6 HCC cell line (Target ratio of 10:1) at 37℃ for 12 hours. Next, all cells were collected for CD45, PI and Annexin V staining and immediate flow cytometry analysis. Percentage of $CD45^-$annexin V^+PI^- (early phase) and $CD45^-$annexin V^+PI^+ (late phase) cells constituted the entire percentage of killed target cells.

Transwell chemotaxis assays

$CD8^+$ T cells with the indicated treatments were allowed to migrate through 5-μm transwell filters (Corning) to the medium in the bottom chamber for 12h, with PBS or tumor CM, were counted by flow cytometry. The following formula was used: chemotaxis index = percentage of migrated cells induced by the indicated chemokine ÷ percentage of migrated cells induced by PBS.

F-actin staining

$CD8^+$ T cells treated with CXCL10 (ABclonal, #RP01642, 100ng/mL) for 15 minutes successively underwent a 15-minute fixation with fresh 4% paraformaldehyde, a 10-minute permeabilization om 0.1% Triton X-100, a 1-hour block with 5% normal goat serum, 15-minute staining with phalloidin FITC (YEASEN, #40735ES75) and DAPI counterstaining before confocal microscopy with a confocal laser-scanning microscope (Leica, #TCS SP8 STED). The Zen Microscope (ZEISS, v2.6) and ImageJ software were used to analyze and quantify F actin staining. All presented images are representative of three independent experiments with at least 30 cells per group. The line-fluorescence-intensity profile of cells was used to define cell polarization. The average fluorescence signal on one side of the polarized cells was more than 1.5 times stronger than that of the opposite side. The frequency of polarized or unpolarized distribution in $CD8^+$ T cells was presented.

Library Preparation and RNA-seq Analysis

Total RNA was extracted from tissues using the RNA-easy Isolation Reagent (Vazyme, #R701-01). A NanoDrop 2000 spectrophotometer (Thermo Scientific) was applied for RNA purity measurement and quantification, and an Agilent 2100 bioanalyzer (Agilent Technologies) was applied for RNA integrity assessment. Sequencing libraries were generated using the TruSeq Stranded mRNA LT Sample Prep Kit (Illumina) following the manufacturer's recommendations. Prepared libraries were sequenced on an Illumina HiSeq X Ten platform. The abundances of transcripts (including mRNAs, pseudogenes, noncoding RNAs, and other predicted RNAs) were calculated and normalized in fragments per kilobase of transcript per million mapped reads. Differential gene expression evaluation was analyzed using R software (v4.2.2).

Single cell RNA-Sequencing and Data analysis

Tissue dissociation and preparation

The fresh tissue was stored in the tissue preservation solution (Singleron Biotechnologies, sCelLiveTM) on ice after the surgery within 30 minutes. The specimens were washed with hanks balanced salt solution (HBSS) for three times, minced into small pieces, and then digested with 3 mL tissue dissociation solution (Singleron, sCelLiveTM) by tissue dissociation system (Singleron, PythoN™) at 37 °C for 15 min. The cell suspension was collected and filtered through a 40-micron sterile strainer. Afterwards, the red blood cell lysis buffer (RCLB, Singleron, GEXSCOPE®) was added, and the mixture (Cell: RCLB=1:2 (volume ratio)) was incubated at room temperature for 5-8 minutes to remove red blood cells. The mixture was then centrifuged at 300 × g 4 ℃ for 5 minutes to remove supernatant and suspended softly with PBS. Finally, the samples were stained with Trypan Blue and the cell viability was evaluated microscopically.

Library Construction and Single Cell RNA-seq Analysis

Single-cell suspensions (2×10^5 cells/mL) with PBS (HyClone) were loaded onto microwell chip using the single cell processing system (Singleron Matrix®). Barcoding Beads are subsequently collected from the microwell chip, followed by reverse transcription of the mRNA captured by the barcoding beads and to obtain cDNA, and PCR amplification. The amplified cDNA is then fragmented and ligated with sequencing adapters. The scRNA-seq libraries were constructed according to the protocol of the Single Cell RNA Library Kits (Singleron, GEXSCOPE®). Individual libraries were diluted to 4 nM, pooled, and sequenced on Illumina novaseq 6000 with 150 bp paired end reads.

Tandem mass tag (TMT)-labeled proteomics

PCT based protein digestion

Cell sample was transferred into a PCT tube. Then 30 μL 6 M Urea/2 M thiourea/100 mM triethylammonium bicarbonate (TEAB), 5 μL 200 mM Tris (2-carboxyethyl) phosphine (TCEP) and 2.5 μL 800 mM iodoacetamide (IAA) was added for reduction and alkylation under 45000 psi, with 30 s high pressure and 10 s ambient pressure per cycle, 30 ℃ for 90 cycles. 75 μL 100Mm TEAB was added into PCT tube to decrease the concentration of Urea to lower than 1.5 M. Then 10 ul Trypsin (0.5 ug/ul), 2.5 ul Lys-C (0.5 ug/ul) were added for protein digestion under 20000 psi, with 50 s high pressure and 10 s ambient pressure per cycle, 30 ℃ for 120 cycles. Tryptic peptides were transferred into 1.5 mL tubes and digestion was then terminated by 15 μL 10% TFA.

Desalting and TMT labeling

Confirm that pH of the samples was between 2 and 3. SOLAμ (Thermo Fisher Scientific™, San Jose, USA) was applied for desalting and TMTpro 16plex Isobaric Label Reagent Set was applied for TMT labeling according to their user guide.

High pH Fractionation

Fractionation was performed with a Waters XBridge Peptide BEH C18 column (300 Å, 5 μm × 4.6 mm × 250 mm) under a DIONEX UltiMate 3000 Liquid Chromatogram. Mobile phase A was 10 mM ammonium hydroxide (pH=10), and mobile phase B was 98% ACN, 10 mM ammonium hydroxide (pH=10). Peptides were collected every one minute from 5% ACN to 35% ACN with a flowrate of 0.5 ml/min in 60 min, and then combined into 30 fractions. After SpeedVac dried, the 30 fraction samples were resuspended with 2% ACN, 0.1% Formic Acid and then sent for LC-MS analysis.

MS analysis

LC-MS/MS with the nanoflow DIONEX UltiMate 3000 RSLCnano System coupled to an Orbitrap Exploris 480 mass spectrometer (Thermo Scientific™, San Jose, USA), which equipped with a FAIMS Pro™ (Thermo Scientific™, San Jose, USA), in data dependent acquisition (DDA) mode. Buffer A. 2% ACN, 98% H2O containing 0.1% FA; Buffer B. 98% ACN in water containing 0.1% FA. All reagents were MS grade for each acquisition, peptides were loaded onto a precolumn (3 μm, 100 Å, 20 mm*75 μm i.d.) at a flowrate of 6 μL/min for 4 min and then injected using a 30 min LC gradient (from 7% to 30% buffer B) at a flowrate of 300 nL/min (analytical column, 1.9 μm, 120 Å, 150 mm*75 μm i.d.). Buffer A was 2% ACN, 98% H2O containing 0.1% FA, and buffer B was 98% ACN in water containing 0.1% FA. All reagents were MS grade. The m/z range of MS1 was 375-1800 with the resolution at 60,000, normalized AGC target of 300% with the intensity threshold of 2e4, and maximum ion injection time (max IT) of 50 ms. MS/MS experiment were performed with a resolution at30000, normalized AGC target of 200%, and max IT of 86 ms. isolation window was set to 0.7 m/z and first mass was set to 110 m/z.

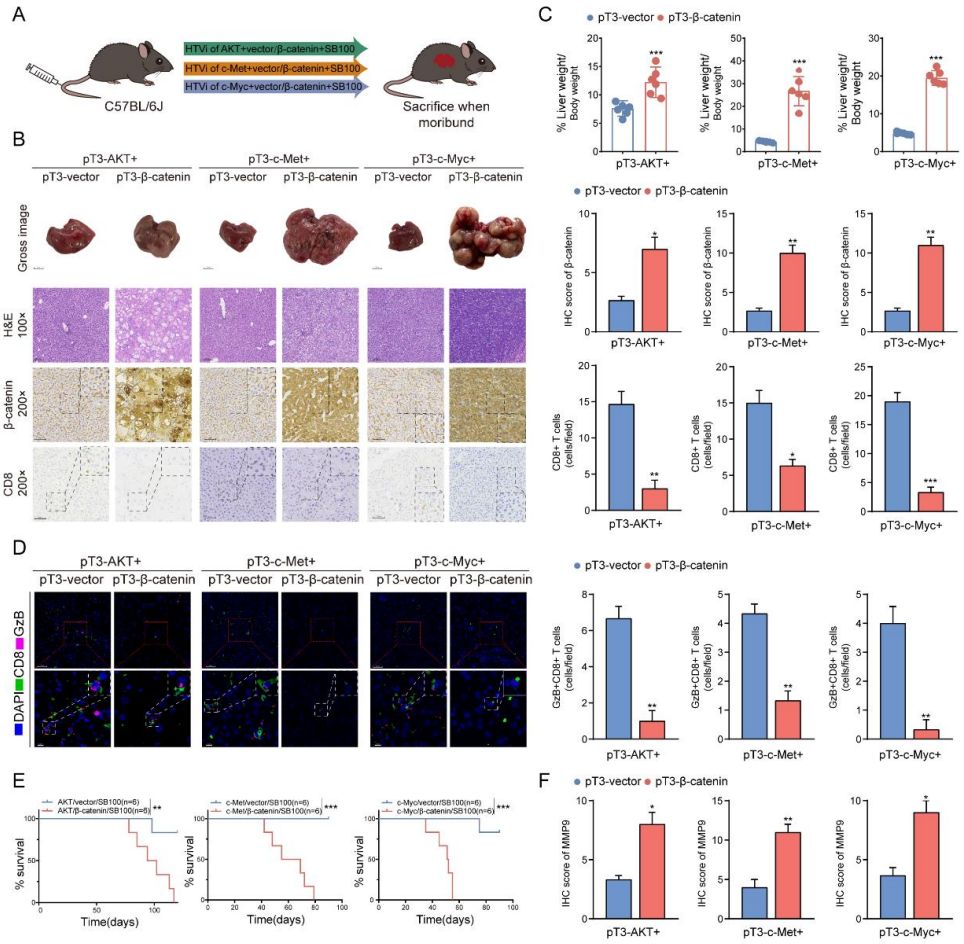

Supplementary Figure S1 Three groups of CTNNB1^{GOF} HCC models were constructed in mice **(A)** Three groups of CTNNB1^{GOF} HCC models were constructed via HTVi of activated AKT (myr-AKT)/β-catenin (ΔN90-β-catenin), c-Met/β-catenin and c-Myc (MYC-IRES-Luc)/β-catenin plasmids. **(B)** Gross images, H&E staining, and IHC staining of β-catenin and CD8 in the three groups of CTNNB1^{GOF} HCC models and statistical analyses. The number of CD8-positive cells per HPF was counted in HCC sections from each group. Three random HPFs were selected for analysis on each slide. **(C)** The liver to body weight ratio of the three groups of CTNNB1^{GOF} HCC models(n=6). **(D)** Representative images of immunofluorescence costaining for CD8 (green) with granzyme B (pink) in the three groups of CTNNB1^{GOF} HCC models and statistical analyses. The number of cells positive for both CD8 and granzyme B per HPF was counted in HCC sections from each group. Three random HPFs were selected for analysis on each slide. **(E)** Survival curves of mice in each group(n=6). **(F)** The IHC staining score analyses of MMP9 in each group. Three random HPFs were selected for analysis on each slide. **P*<0.05, ***P*<0.01, ****P*<0.001. Mean±SEM. Unpaired Student's t-test(B,C,D,F), log-rank test(E). CTNNB1^{GOF}, gain of function mutations in CTNNB1; IHC, immunohistochemistry; HPF, high-power field.

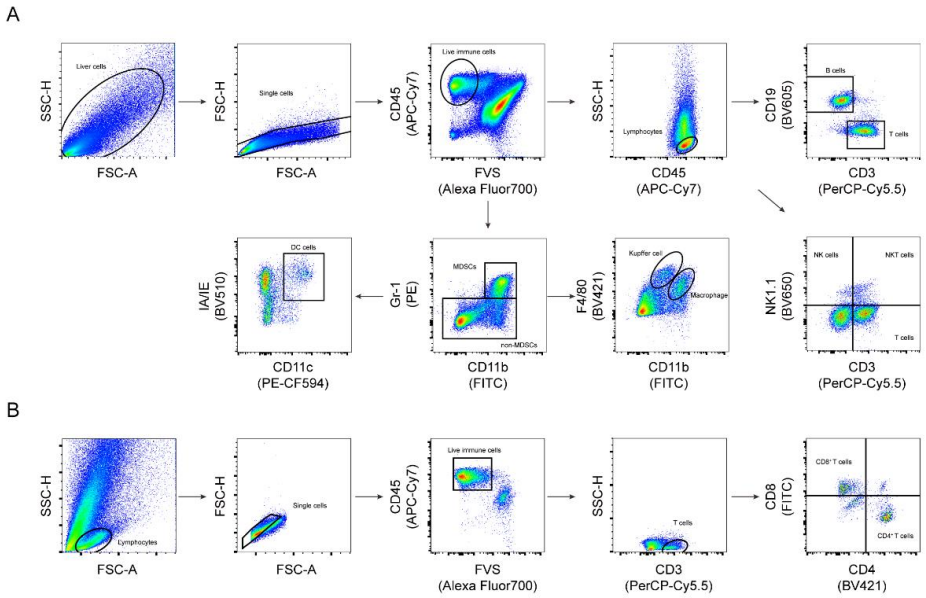

Supplementary Figure S2 Flow cytometry analysis of liver immune microenvironment in the three groups of CTNNB1^{GOF} HCC models

(A, B) The gate method of live hepatic CD45^{+} cells.

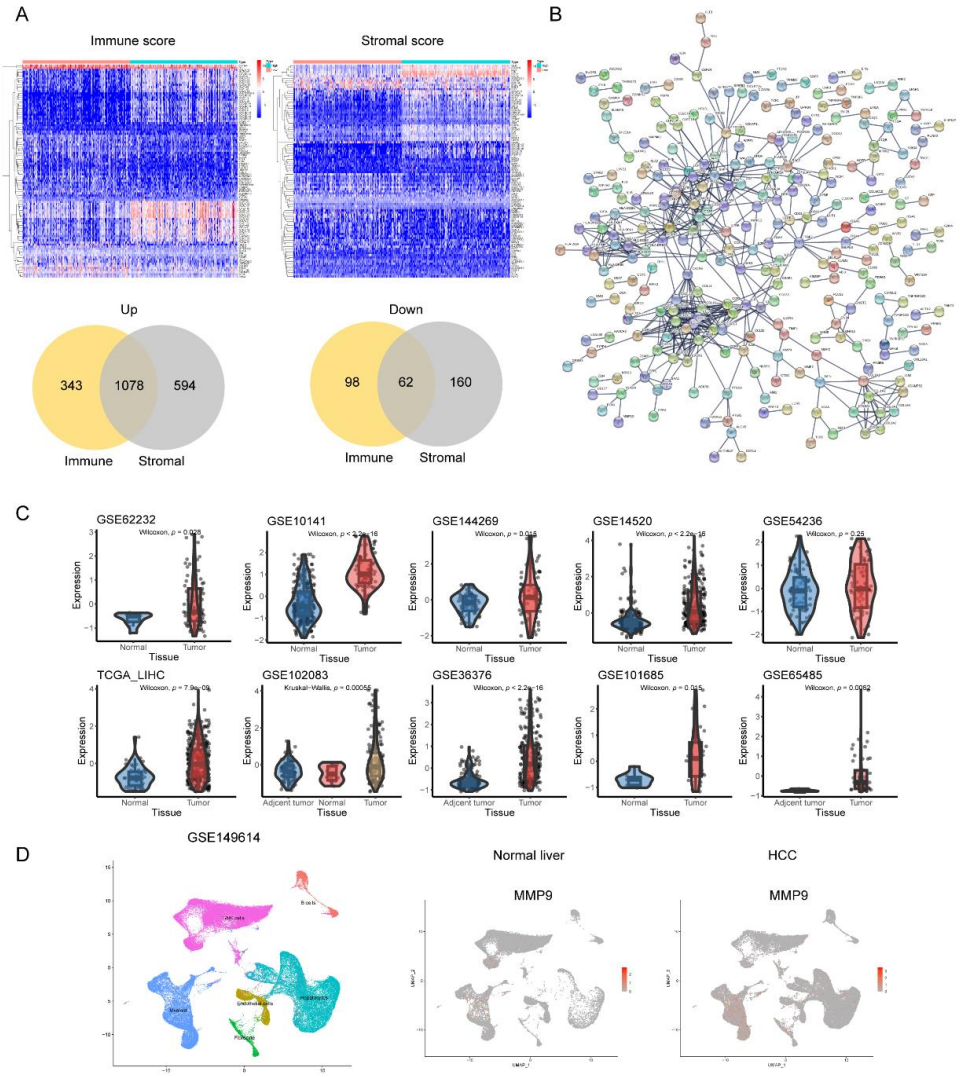

Supplementary Figure S3 Bioinformatics analyses of public database data

(A) The heatmap and Venn diagram of DEGs screened by ImmuneScore and StromalScore analysis in TCGA dataset. **(B)** The PPI network diagram of genes associated with immune regulation. **(C)** The mRNA expression of MMP9 in normal liver and HCC tissue in GEO datasets. **(D)** Analysis of MMP9 gene expression in various cells using *Lu*'s single cell expression data. TCGA, The Cancer Genome Atlas; DEGs, differentially expressed genes; GEO, Gene Expression Omnibus; PPI, Protein–protein interaction.

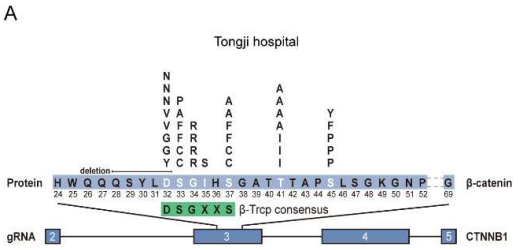

Supplementary Figure S4 Spectrum of CTNNB1 exon3 mutations in HCC

(A) Mutations in CTNNB1 exon3 identified in HCC Tongji cohort. Amino acid substitutions and small in-frame deletions identified in the tumors are shown above the human β-catenin amino acid sequence.

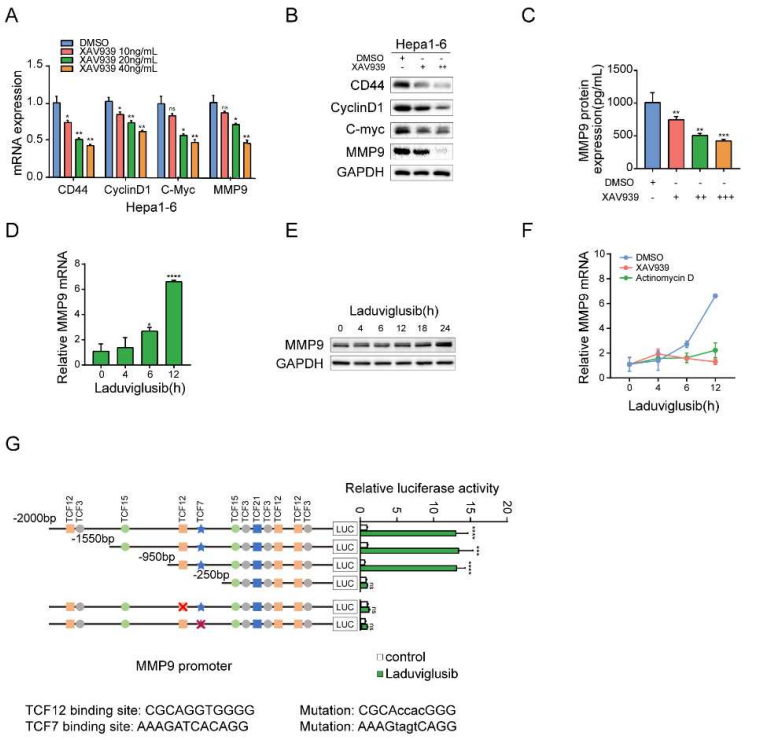

Supplementary Figure S5 Wnt/β-catenin signal regulates MMP9 transcription in HCC in *vitro*

(A) Hepa1-6 cells were treated with Wnt/β-catenin signature inhibitor XAV939 (10/20/40 ng/mL) or DMSO. The mRNA expression of CD44, CyclinD1, c-myc and MMP9 were measured by qRT-PCR. **(B)** Hepa1-6 cells were treated with XAV939(10/20 ng/mL) or DMSO followed by western blotting to detect the expression of CD44, CyclinD1, c-myc and MMP9. **(C)** Hepa1-6 cells were treated with XAV939(10/20/40 ng/mL) or DMSO followed by Elisa to detect the MMP9 secretion level from culture medium supernatant. **(D)** Hepa1-6 cells were treated with Wnt/β-catenin activator laduviglusib (10 ng/mL). The mRNA expression of MMP9 were measured by qRT-PCR. **(E)** Hepa1-6 cells were treated with laduviglusib (10 ng/mL) followed by western blotting to detect the expression of MMP9. **(F)** Time course of MMP9 mRNA levels in Hepa1-6 cells treated with laduviglusib (10 ng/mL), together with XAV939 (20 ng/mL) or actinomycin D (1 mg/mL). **(G)** Activities of MMP9 promoter truncations or mutations in laduviglusib-β-treated Hepa1-6 cells were measured by dual-luciferase assays. **P*<0.05, ***P*<0.01, ****P*<0.001, *****P*<0.0001. Mean±SEM. Unpaired Student's t-test(A,C,D,F,G). qRT-PCR, quantitative real-time PCR.

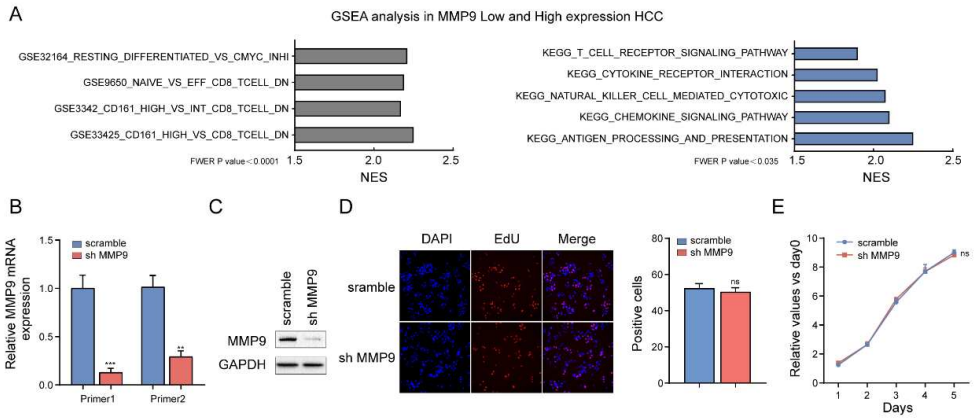

Supplementary Figure S6 MMP9 had little impact on HCC proliferation in *vitro*

(A) GESA analysis in MMP9 low and high expression HCC obtained from the TCGA dataset. **(B, C)** qRT-PCR and western blotting analyses of MMP9 knockdown efficiency in Hepa1-6 cell line. **(D, E)** EdU and CCK-8 experiments were used to verify the effect of MMP9 on proliferation capability. ns, no significance, ***P*<0.01, ****P*<0.001. Mean±SEM. Unpaired Student's t-test(B,E). GSEA, Gene Set Enrichment Analysis; qRT-PCR, quantitative real-time PCR; CCK8, Cell Counting Kit-8.

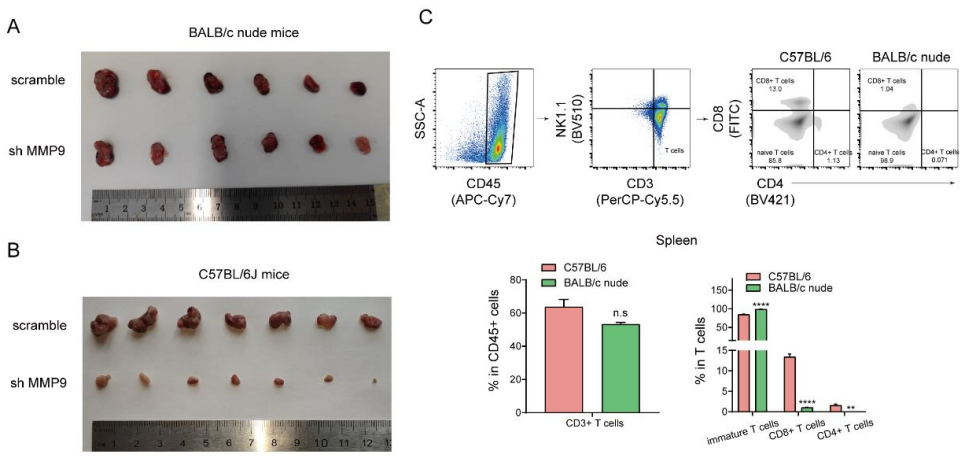

Supplementary Figure S7 Knockdown of MMP9 significantly suppressed HCC progression in C57BL/6J mice but not in BALB/c nude mice

(A, B) Gross images of Hepa1-6 (scramble/sh MMP9) subcutaneous tumors in BALB/c nude mice and C57BL/6J mice. **(C)** Representative flow cytometry data showing the proportion of T cells in spleens from C57BL/6J mice and BALB/c nude mice. The statistics results are shown below(n=5). ns, no significance, *P<0.05, **P<0.01, ****P<0.0001. Mean±SEM. Unpaired Student's t-test(C).

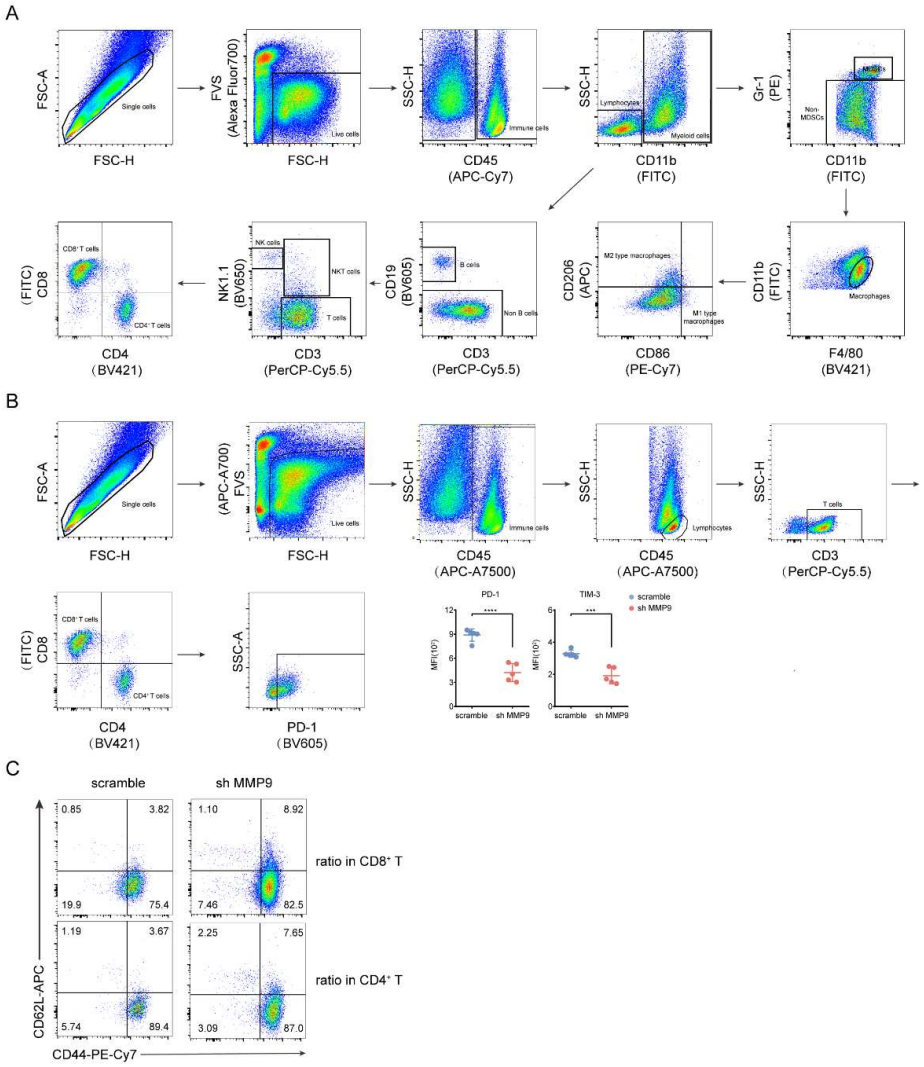

Supplementary Figure S8 Flow cytometry analysis of liver immune microenvironment in orthotopic tumor tissue from C57BL/6 mouse models

(A) The gate method of live hepatic $CD45^+$ cells. **(B, C)** The gate method of ICB (PD-1, TIM-3, CTLA-4 and LAG-3) positive T cells and immune memory ($CD44^{lo}$ $CD62L^{hi}$, $CD44^{hi}$ $CD62L^{lo}$ and $CD44^{hi}$ $CD62L^{hi}$) T cells. ICB, immune checkpoint blockade; PD-1, programmed death-1; TIM-3, t cell immunoglobulin and mucin domain-3.

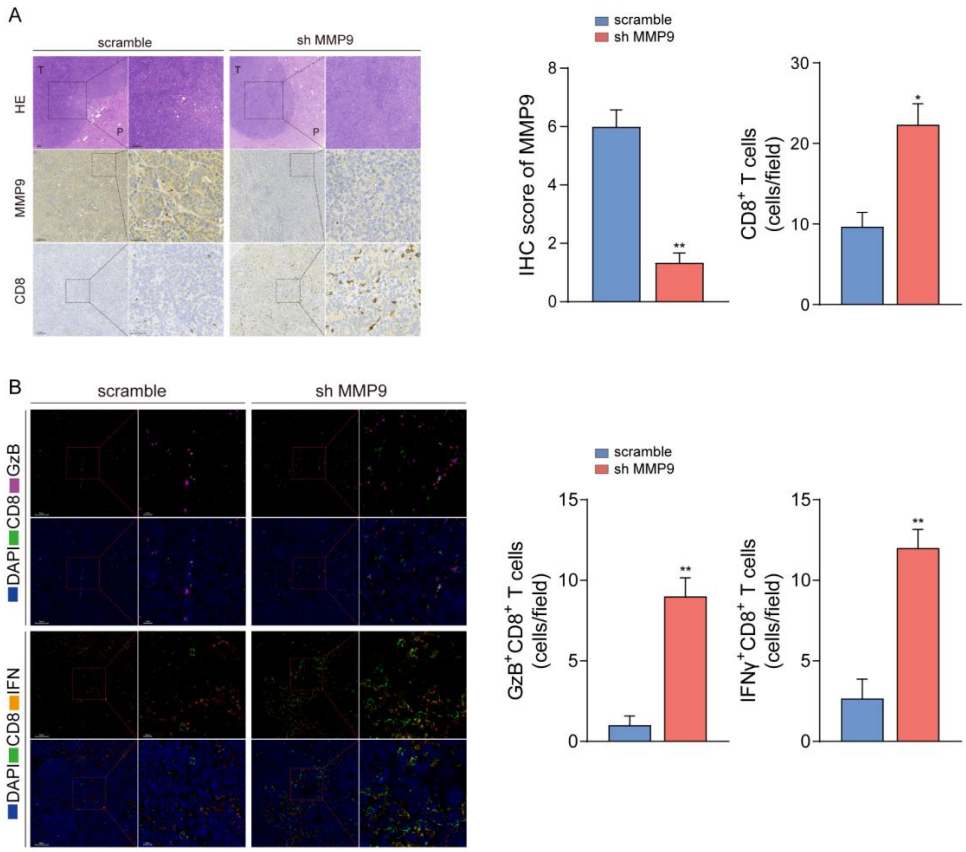

Supplementary Figure S9 Knockdown of MMP9 enhances cytotoxicity of CTLs

(A) H&E staining and IHC staining of MMP9 and CD8 in orthotopic tumor tissue from C57BL/6 mouse models and statistical analyses. The number of CD8-positive cells per HPF was counted in HCC sections from each group. Three random HPFs were selected for analysis on each slide. **(B)** Representative images of immunofluorescence costaining for CD8 (green) with granzyme B (violet) or IFN-γ (orange) in orthotopic tumor tissue from C57BL/6 mouse models and statistical analyses. The number of cells positive for both CD8 and granzyme B or IFN-γ per HPF was counted in HCC sections from each group. Three random HPFs were selected for analysis on each slide. **P*<0.05, ***P*<0.01. Mean±SEM. Unpaired Student's t-test(A,B). IFN-γ, interferon γ.

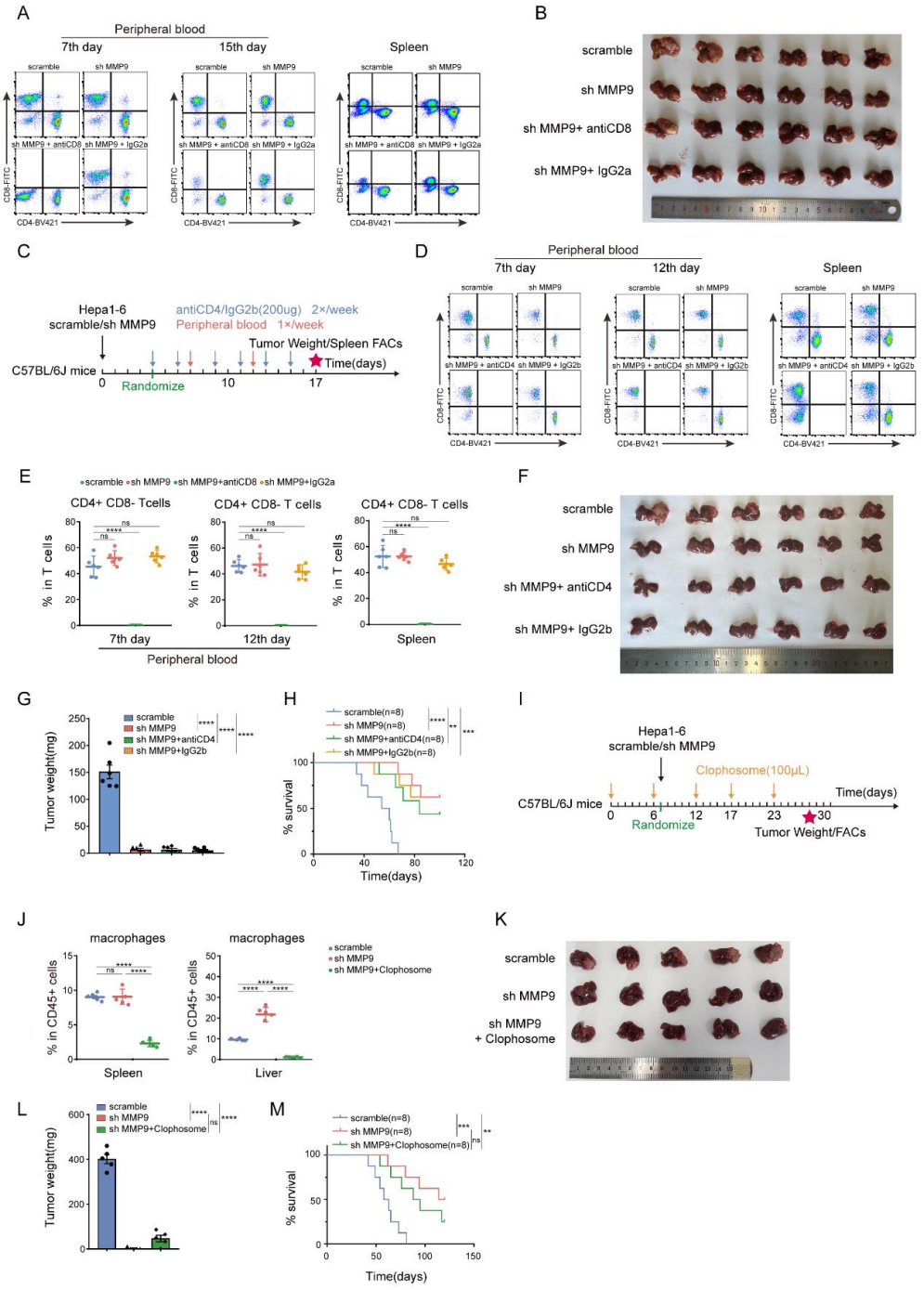

Supplementary Figure S10 MMP9 promotes HCC progression through CD8$^+$ T cell-dependent rather than CD4$^+$ T cell or macrophage-dependent mechanisms

(A) Representative flow cytometry data showing the proportion of CD8$^+$ T cells from peripheral blood and spleen tissue. **(B)** Gross images of Hepa1-6 tumors in C57BL/6J mice (CD8-neutralizing antibodies, 200 μg/mice; IgG2a, 200 μg/mice). **(C)** Schematic representation of the treatment schedule for CD4-neutralizing antibodies or IgG2b. **(D)** Representative flow cytometry data

showing the proportion of $CD4^+$ T cells from peripheral blood and spleen tissue. **(E)** Flow cytometry analysis of depletion efficiency of $CD4^+$ T cells from peripheral blood and spleen tissue. **(F)** Gross images of Hepa1-6 tumors in C57BL/6J mice (CD4-neutralizing antibodies, 200 μg/mice; IgG2b, 200 μg/mice). **(G)** The tumor weight of C57BL/6J mouse models (CD4-neutralizing antibodies, 200 μg/mice; IgG2b, 200 μg/mice, n=6). **(H)** Survival curves of mice in each group of C57BL/6J mouse models (n=8). **(I)** Schematic representation of the treatment schedule for clophosome (macrophage scavenger). **(J)** Flow cytometry analysis of depletion efficiency of macrophages from spleen and liver tissue. **(K)** Gross images of Hepa1-6 tumors in C57BL/6J mice (1.4mg first day, 0.7mg every 6 days). **(L)** The tumor weight of C57BL/6J mouse models (clophosome, 100 μL/mice, n=5). **(M)** Survival curves of mice in each group of C57BL/6J mouse models (n=8). ns, no significance, $^{**}P<0.01$, $^{***}P<0.001$, $^{****}P<0.0001$. Mean ± SEM. One-way ANOVA with Tukey's multiple comparisons test(E, G, J, L), log-rank test(H, M). FACs, Fluorescence-activated cell staining.

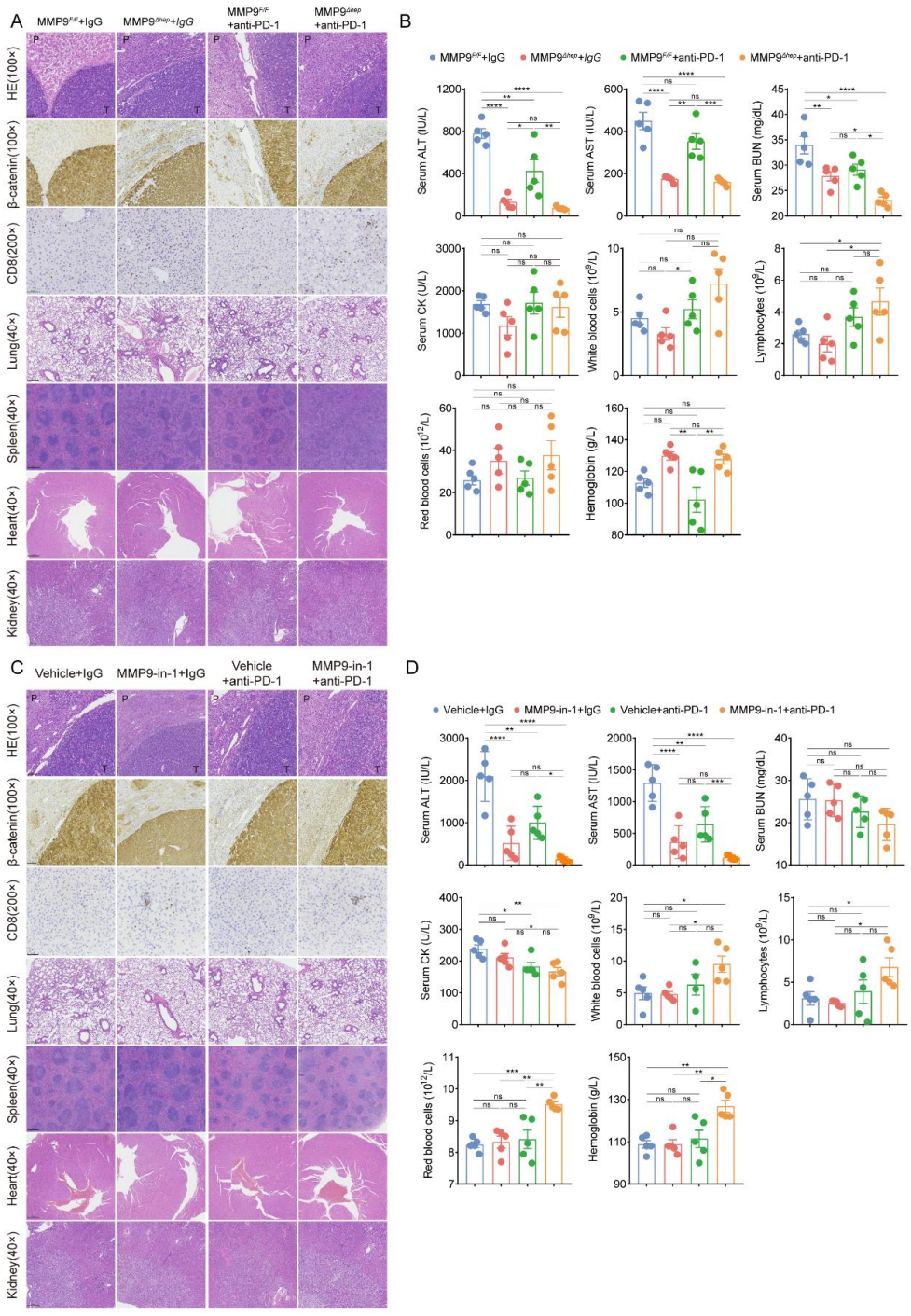

Supplementary Figure S11 The safety of combination therapy was validated through H&E staining, IHC, blood routine and blood biochemistry test analyses

(A) H&E staining and IHC staining of β-catenin and CD8 in the four groups of spontaneous HCC models driven by c-Myc/β-catenin (MMP9$^{F/F}$ + IgG; MMP9$^{\Delta hep}$ + IgG; MMP9$^{F/F}$ + anti-PD-1; MMP9$^{\Delta hep}$ + anti-PD-1, anti-PD-1, 200 μg/mice; IgG, 200 μg/mice). **(B)** Blood routine and blood biochemistry test analyses of four groups of spontaneous HCC models driven by c-Myc/β-catenin

(MMP9$^{F/F}$ + IgG; MMP9$^{\Delta hep}$ + IgG; MMP9$^{F/F}$ + anti-PD-1; MMP9$^{\Delta hep}$ + anti-PD-1, n=5). **(C)** H&E staining and IHC staining of β-catenin and CD8 in the four groups of spontaneous HCC models driven by c-Myc/β-catenin (Vehicle+ IgG; MMP9-in-1 + IgG; Vehicle + anti-PD-1; MMP9-in-1*p* + anti-PD-1, MMP9-in-1, 20mg/kg; anti-PD-1, 200 μg/mice; IgG, 200 μg/mice). **(D)** Blood routine and blood biochemistry test analyses of four groups of spontaneous HCC models driven by c-Myc/β-catenin (Vehicle+ IgG; MMP9-in-1 + IgG; Vehicle + anti-PD-1; MMP9-in-1*p* + anti-PD-1, n=5). ns, no significance, **P*<0.05, ***P*<0.01, ****P*<0.001, *****P*<0.0001. Mean±SEM. One-way ANOVA with Tukey's multiple comparisons test(B,D).

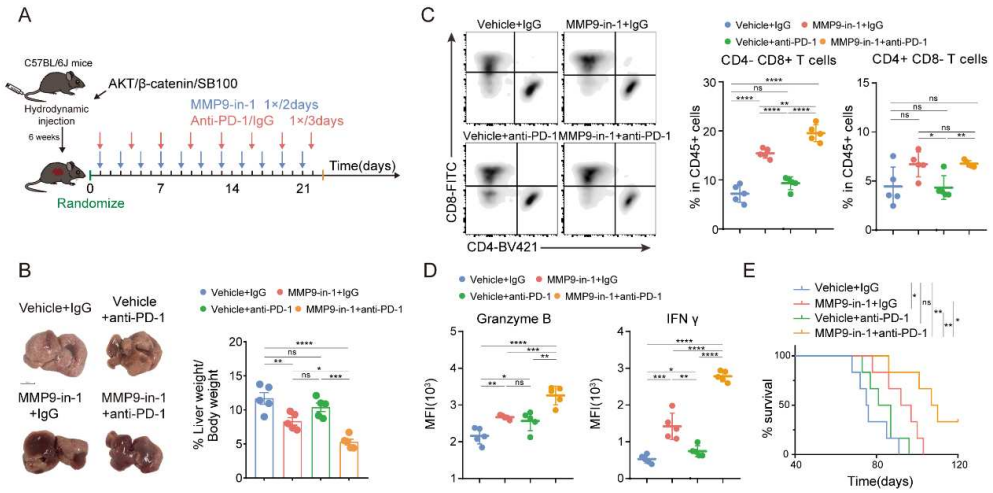

Supplementary Figure S12 MMP-9-in-1 sensitizes the efficacy of the anti-PD-1 antibody in spontaneous HCC models driven by Akt/β-catenin

(A) Schematic representation of the therapy schedule for MMP9-in-1, anti–PD-1 or combination therapy. **(B)** Representative images and the statistical results from spontaneous HCC models driven by Akt/β-catenin that received the indicated treatments (MMP9-in-1, 20mg/kg; anti-PD-1, 200 μg/mice; IgG, 200 μg/mice, n=5). **(C)** Representative flow cytometry data showing the proportion of T cells in tumor tissue from spontaneous HCC models. The statistics results are shown on the right. **(D)** The statistics results of MFI of granzyme B and IFN-γ on $CD8^+$ T cells in tumor tissue from spontaneous HCC models. **(E)** Survival curves of mice in each group of spontaneous HCC models (n=6). ns, no significance, **P*<0.05, ***P*<0.01, ****P*<0.001, *****P*<0.0001. Mean±SEM. One-way ANOVA with Tukey's multiple comparisons test(B, C, D), log-rank test(E).

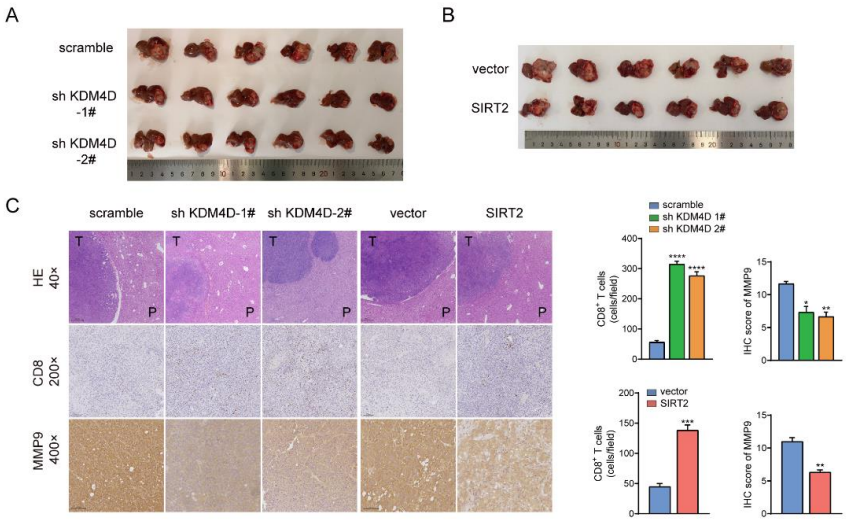

Supplementary Figure S13 KDM4D knockdown and SIRT2 overexpression suppressed MMP9 expression and infiltration of CD8$^+$T cells

(A, B) Gross images of Hepa1-6 (scramble/sh KDM4D or vector/SIRT2) tumors in C57BL/6J mice. **(C)** H&E staining and IHC staining of MMP9 and CD8 in orthotopic tumor tissue from C57BL/6J mouse models and statistical analyses. The number of CD8-positive cells per HPF was counted in HCC sections from each group. Three random HPFs were selected for analysis on each slide. **P*<0.05, ***P*<0.01, ****P*<0.001. Mean±SEM. Unpaired Student's t-test(C).

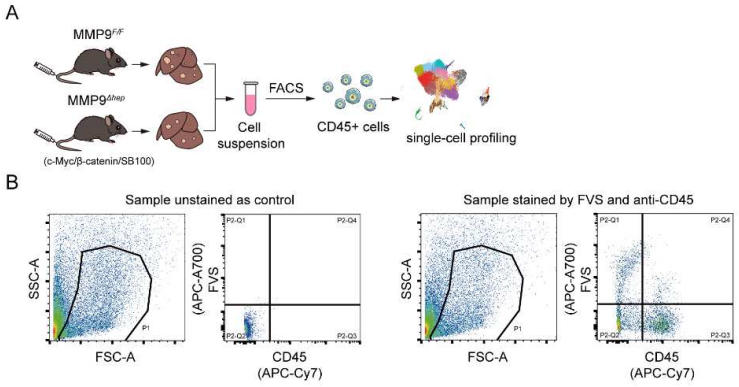

Supplementary Figure S14 Sample preparation and sorting strategy for single-cell sequencing **(A)** Schematic representation of the experimental strategy. **(B)** Two-dimensional scatterplot, showing the gating strategy used to sort live $CD45^+$ immune cells (P2-Q3 in the right panel). Sorted cells were used as the template for single-cell RNA preparations.

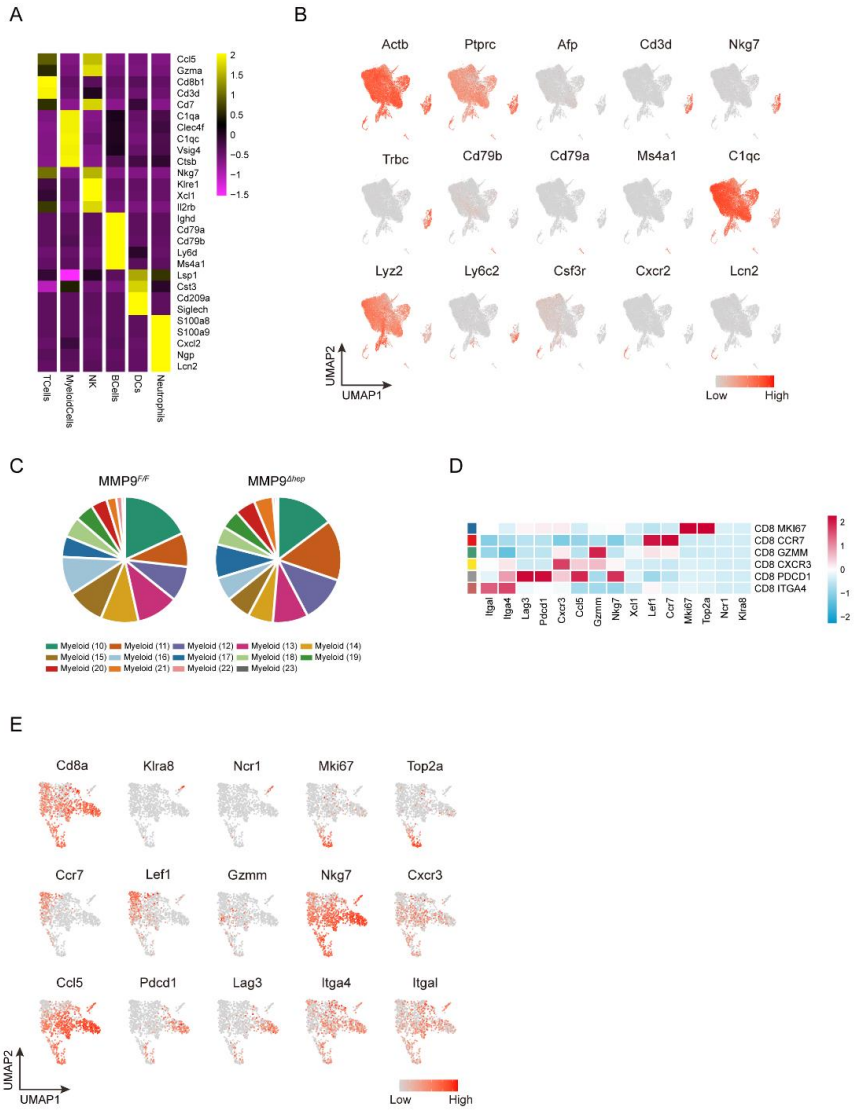

Supplementary Figure S15 Single-cell sequencing profiling of the ecosystem in MMP9$^{F/F}$ and MMP9$^{\Delta hep}$ mice HCC samples

(A) Heatmap showing the expression of marker genes in the indicated cell types. **(B)** UMAP plot showing the expression levels of marker genes, defined for all cell types. **(C)** Tortadiagram indicating the proportion of myeloid immune cells. **(D)** Heatmap showing the expression of marker genes in the indicated CD8$^+$ cell types. **(E)** UMAP plot showing the expression levels of marker genes, defined for all CD8$^+$ cell types.

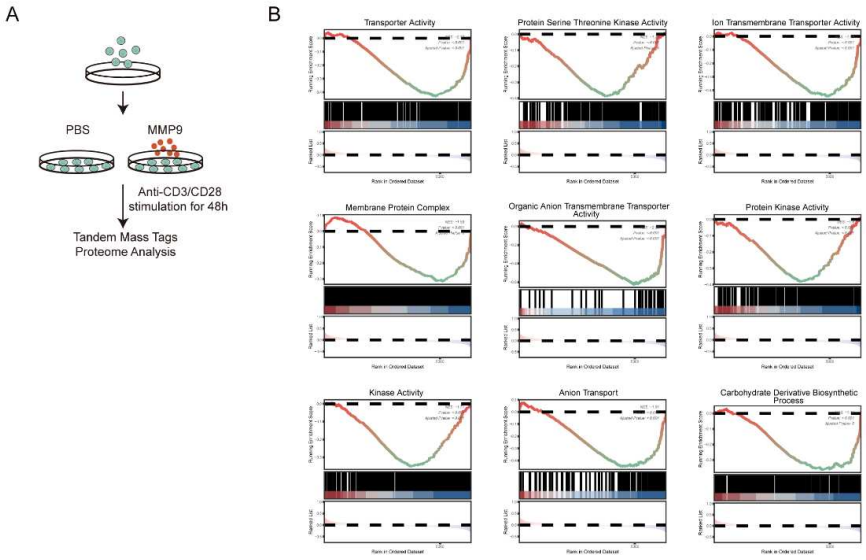

Supplementary Figure S16 MMP9 stimulation was associated with a variety of membrane transport processes of CD8$^+$ T cells

(A) Schematic representation of the experimental strategy. **(B)** GSEA of proteomics data revealed that MMP9 inhibits various of transporter activities on the cell membrane of CD8$^+$ T cells.

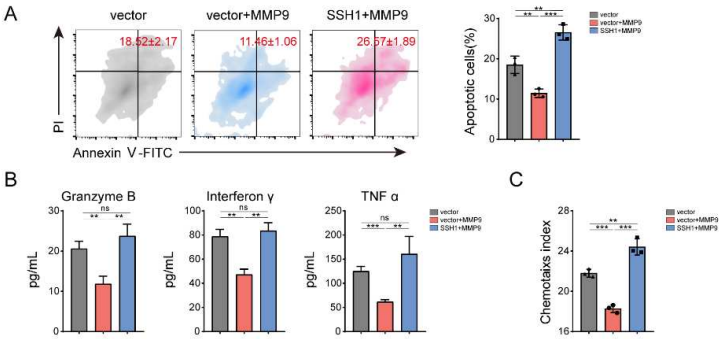

Supplementary Figure S17 SSH1 upregulation abrogated the suppression of migration and activation of CD8$^+$ T cells induced by MMP9

(A) Apoptosis of Hepa1-6 cells caused by CD8$^+$ T cells (vector/vector+MMP9/SSH1+MMP9) was measured using Annexin V - PI staining. **(B)** CD8$^+$ T cells (vector/vector+MMP9/SSH1+MMP9) followed by Elisa to detect the granzyme B, IFN-γ and TNFα secretion level from culture medium supernatant. **(C)** CD8$^+$ T cells (vector/vector+MMP9/SSH1+MMP9) were determined by the transwell assay, and the chemotaxis index is shown. ns, no significance, ***P*<0.01, ****P*<0.001. Mean±SD. One-way ANOVA with Tukey's multiple comparisons test(A,B,C).

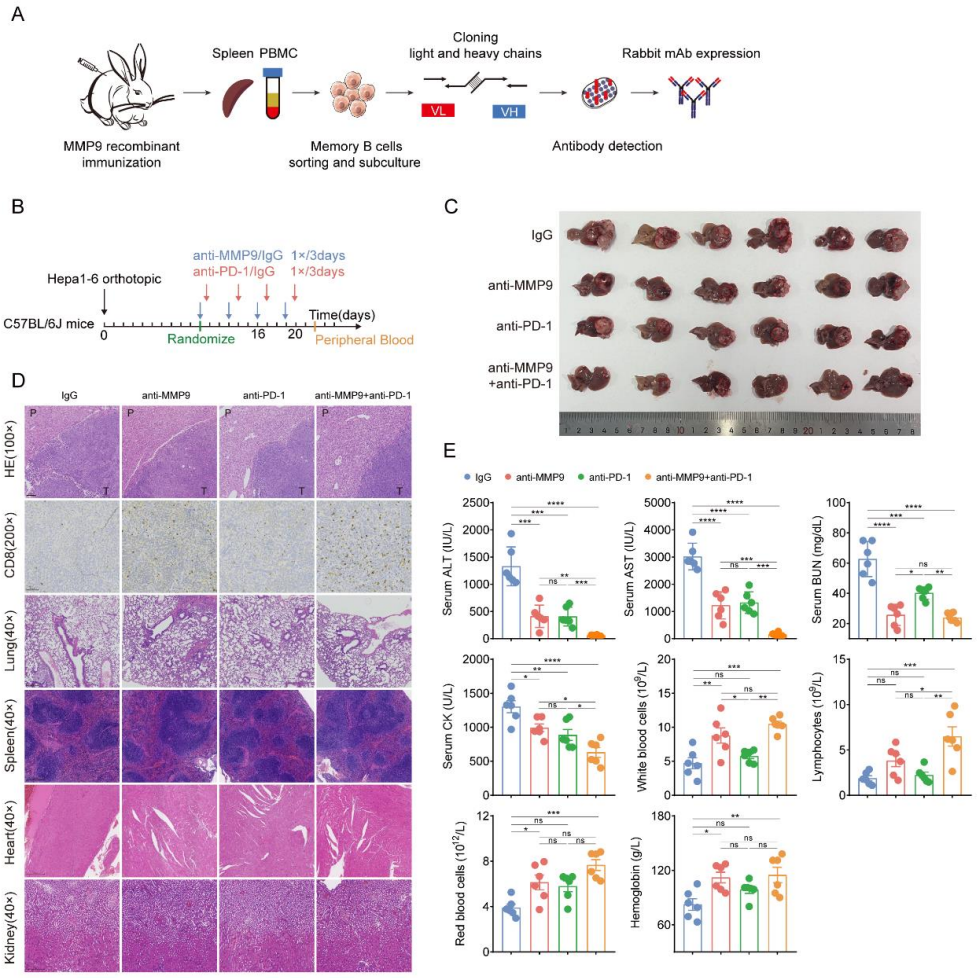

Supplementary Figure S18 The anti-MMP9 antibody sensitizes the efficacy of the anti-PD-1 antibody

(A) Schematic representation of the anti-MMP9 rabbit monoclonal antibody development strategy. **(B)** Schematic representation of the therapy schedule for anti-MMP9, anti–PD-1 or combination therapy. **(C)** Representative images of Hepa1-6 orthotopic models that received the indicated treatments (anti-MMP9, 200 μg/mice; anti-PD-1, 200 μg/mice; IgG, 200 μg/mice, n=6). **(D)** H&E staining and IHC staining of CD8 in the four treatment groups of Hepa1-6 orthotopic models. **(E)** Blood routine and blood biochemistry test analyses in the four treatment groups of Hepa1-6 orthotopic models. **P*<0.05, ***P*<0.01, ****P*<0.001, *****P*<0.0001. Mean±SEM. One-way ANOVA with Tukey's multiple comparisons test(E).

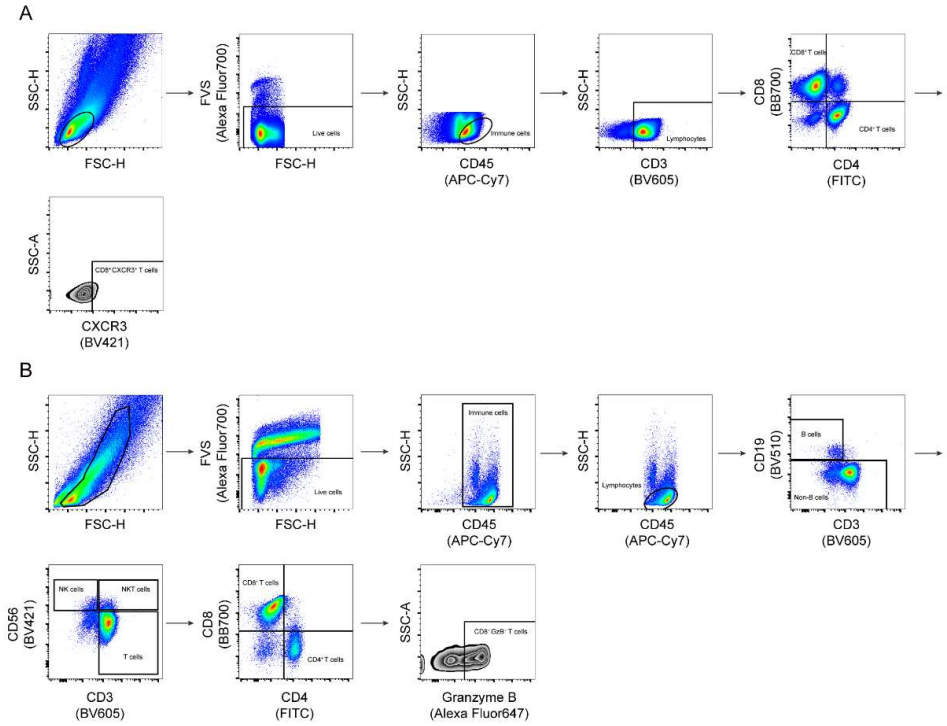

Supplementary Figure S19 Flow cytometry analysis of primary HCC surgical samples

(A) The gate method of $CD8^+$ $CXCR3^+$ T cells. (B) The gate method of $CD8^+$ Granzyme B^+ T cells.

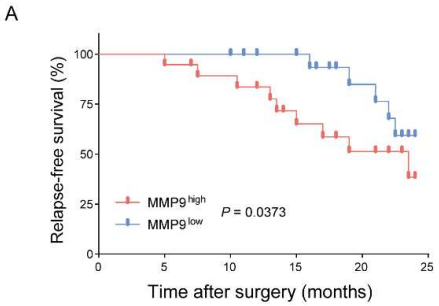

Supplementary Figure S20 Relapse-free survival rate of patients after surgery.

(A) Patients received anti-PD-1 adjuvant therapy after hepatectomy (n=38). Patients were re-examined every 3 months and evaluated within two years.

Supplementary Table S1 Up-regulated genes in the three groups of spontaneous tumor compared with the corresponding control groups

	AKT/β-catenin		C-Met/β-catenin		C-Myc/β-catenin	
gene	logFC	*P* value	logFC	*P* value	logFC	*P* value
MMP9	1.569675	0.004823	2.936847	4.86E-06	4.238257	0.002186
PROCR	1.323703	0.02475	1.651422	0.0359	1.521154	0.041868
ZFP287	2.708681	0.009018	2.477729	0.020458	2.487976	0.019315

Supplementary Table S2 DEGs screened by ImmuneScore and StromalScore

Gene	logFC	Gene	logFC	Gene	logFC	Gene	logFC	Gene	logFC	Gene	logFC
AL133371.2	1.441901	ZEB2	1.522461	LAPTM5	1.565254	IGLC7	3.717952	IGHV1-69	3.328531	TMEM154	1.126085
NTRK2	1.816134	ADAM28	2.11929	IGKV1-17	2.472821	CCL22	2.047568	FPR1	2.23156	IGKV2-24	2.598572
FCRLA	1.563188	VCAN	1.45213	IGFBP5	1.643704	CD200R1	1.502807	AC119044.1	1.68193	GPR183	1.56834
PTPRO	1.181313	TRGV4	1.734227	PLEK	1.652294	TRAV8-2	1.969247	L1CAM	1.523234	TRBV4-1	2.485857
CRIP1	1.393638	TRAV41	1.933954	GBP5	2.954482	ITGAX	1.337363	SLAMF6	2.076265	RGS1	1.635601
CXCR4	1.363235	AXL	1.488011	GPR132	1.75521	MAP1LC3C	2.270881	JAK3	1.685545	CCDC80	2.789447
CXorf21	1.541721	TNC	1.999432	COL6A3	1.685263	ITGB2-AS1	1.572501	MXRA5	2.33682	STX11	1.349317
IGHA2	2.732329	RPLP0P2	1.227309	MMP2	2.367645	IGKV1D-13	3.296649	TMEM132E	1.725107	PARVG	1.61097
PODNL1	1.797807	CXCR2	1.68471	RUNX2	1.743533	HSPB7	1.705654	AC010457.1	1.893478	AP000812.1	1.293043
TRBV14	1.796614	TRARG1	7.666055	ADAMTS2	1.845301	CD69	1.758198	SIGLEC7	1.713317	FOSL1	1.400132
MYO1F	1.391788	C16orf54	1.834491	FMOD	1.601351	BOC	1.474073	IGHD	3.025001	BMPER	1.859776

SSPN	1.342085	INPP5D	1.146359	UNC5C	1.531202	DCSTAMP	1.394283	CD74	1.422059	ALOX5	1.126461
IL2RA	2.119479	SLAMF1	1.773307	CCL5	1.995192	KLRB1	1.598851	PDCD1LG2	2.062507	MIR155HG	1.725158
JPH2	1.92918	GLIPR2	1.597588	PTPN22	1.792271	CSF3R	1.442954	CTSW	1.708773	DPT	2.641786
WFDC1	1.746317	AC002091.1	1.656972	HK3	1.6743	C1QTNF2	1.572539	IGLV4-69	3.610535	SLC7A8	1.310126
FCRL3	2.35091	S100A4	1.491833	LCP1	1.289237	TPSAB1	1.823242	MS4A4A	1.553765	MT1M	1.21925
DOCK10	1.225422	ADAMTS12	1.638548	IGLV3-19	2.9739	PCED1B-AS1	1.809299	RCSD1	1.41193	IGHV3-74	3.154936
TNFRSF17	2.586948	HSPB6	1.310985	APOBEC3H	1.403482	TCN1	1.948444	GAS1	2.085233	CRYBB1	3.543086
LINC02273	2.000444	PLN	2.971688	GIMAP4	1.293074	RCAN2	1.628895	SNCA	1.238666	PCDHGA12	1.689477
MS4A1	3.223866	TRAV39	2.055671	RIPK3	1.205112	UCP2	1.319903	CXCL8	1.564398	CD96	1.748744
MEOX1	1.918685	BMP5	2.010179	AL357054.4	1.121117	FCN1	1.595153	PTGER4	1.260516	PDE1A	1.587698
COL14A1	2.125554	DAPP1	1.96635	CXCL1	1.554354	CD4	1.079918	IGHG4	2.385577	CSF1R	1.590705
HLA-DQB2	1.800013	LSP1	1.505788	AC109479.1	1.798081	DCLK1	2.430988	GBP4	1.253526	HAND2-AS1	2.64553
PDPN	2.829737	LINC00861	1.868206	ADCY7	1.125865	TRBV7-3	2.171242	HLA-DPA1	1.746268	ITGB2	1.722443
FGL2	1.628732	SLAMF8	2.000595	FOLR2	1.397238	RASAL3	1.40969	C7	2.42048	LGALS9	1.092214
GZMH	1.48586	HLA-DRB5	1.62778	APOBEC	1.61253	MARCO	2.96584	GAPT	2.08426	MFAP4	2.59656

	5		4	3C	5		4		4		
ABI3	1.28883 5	LYVE1	1.07531 9	IGHG1	2.61784 8	COL10A1	2.58162 6	LPAR1	1.43679 5	CCL21	3.10261 5
SLC8A1	1.49010 1	IGHV3-30	2.58540 9	IGHV3-64	3.45118 7	KCNK6	1.21092 7	IGSF6	1.41501 8	CDH11	1.95100 1
RNASE6	1.48789 2	CD53	1.85157 6	CXCR2P1	1.87984 4	SMPD3	1.26672 7	S100A12	1.07402 9	PDZRN3	1.47071 6
AREG	1.31359	TRBV15	2.20489 4	CD6	1.94865 7	CARMIL2	1.49065 8	CYP4F29P	1.74480 6	UBASH3A	1.98224 1
MMP25	1.35936 9	LCP2	1.58633	GSDMA	1.63703 8	SLA	1.79963 7	OMG	3.97756 2	VAV1	1.72281 9
LST1	1.41309 3	TRAV13-2	1.85421 2	ITGA4	1.59846 8	FNDC1	2.32335 6	AP002358.2	1.24807 7	COLEC10	2.00392 7
C5AR1	1.15039 1	SFRP4	2.02104 3	IL34	1.22356 4	GPR18	1.82653 5	CPNE5	1.32883 5	LINC01914	1.18924 6
IGHV1-45	2.67679 9	PTGDR	1.37483 6	HRH1	1.31072 3	MS4A14	1.27256	ICOS	2.00068 9	BCL2A1	1.57516 6
NAPSB	1.72578 2	IGLV2-28	2.51568	KLK10	3.00374	STAP1	1.86636 3	LILRA2	1.42892 7	PLCB2	1.46135 1
IGKV3D-11	3.23963 6	ST8SIA4	1.28636 4	IGLC2	2.50039	ADRA2A	2.10754 1	TRAV12-3	2.01250 5	HLA-DRB1	1.71946 1
CD209	1.33551 7	HLA-DPA3	1.31476 6	AC135068.2	3.41711 1	TRBV19	2.13605 2	SLA2	1.74637 1	HTRA4	1.98645 5
PTGIR	1.63432 3	DOK3	1.20519 2	NTF3	1.40778 5	EFNB3	1.49002 8	ACAP1	1.38640 2	C1QTNF7	2.08803 7
PIK3CD	1.64376 1	IGKV2-30	3.19128 5	LCK	1.94162 7	MS4A7	1.57266 8	TRBV9	2.18013 8	AOAH	1.69710 3
COX7A1	2.03673 8	CLEC4G	2.67448 7	IGHJ2	2.49797 8	IL13RA2	2.30563 5	IL11	4.00937 8	KCNA3	2.11511 1
GZM	2.55	IGKV	2.17	SLC6	1.13	CD30	1.41	LILR	1.54	CD1E	1.66

K	2426	1-8	4125	A6	3483	0E	5301	B2	8061		1554
CCR4	1.939127	MXRA8	1.847805	IL21R	2.296707	F13A1	1.811261	BIRC3	1.413095	PRKCB	1.70616
TBXAS1	1.385272	CRHBP	2.00058	KCNE4	1.524633	IGKV1-39	2.667953	FLT3	1.628064	TRGC2	1.803035
SMIM25	1.708811	EBI3	1.47255	IGHV5-78	1.63961	IGHV3-7	2.758996	TNFSF8	1.739256	CXCR3	1.93649
MZB1	2.458488	LRRC15	2.66467	BTLA	2.115933	GALNT17	1.381029	SAA2-SAA4	1.683503	WIPF1	1.299368
EGFL6	1.3872	LRRK1	1.27713	TRBV12-3	1.733506	RHOH	1.469616	SELPLG	1.763457	HACD4	1.380182
LY75	1.333551	ECM1	1.423008	SELP	1.712085	LRRN3	1.820988	GIMAP1	1.265862	TNFAIP8L2	1.42868
AC018755.4	1.718362	TRAV26-1	2.253326	ATP2A3	1.441532	EMILIN1	2.047116	GEM	1.862358	TRBV20-1	2.089902
IGKV3D-15	3.642963	TMEM119	2.479888	FBLN2	2.285793	AC018529.1	1.696053	IGKV4-1	2.776771	TRAV21	2.097588
SRGN	1.52376	SYNPO2	1.543889	LOXL1-AS1	1.216855	FZD2	1.275776	SLC9A9	1.474379	TMEM26	1.455501
TIMP1	1.326685	SPIC	1.423369	HLA-DRB9	1.633254	SH2D1A	2.096343	CMKLR1	1.613157	TRBV7-9	2.239413
PRKCQ	1.77699	RPL29P19	1.800642	TRBJ2-3	1.882828	IL7R	2.508129	OMD	2.601424	ITGA9	1.425604
CEMIP	1.204921	PLAUR	1.529006	C1QA	1.683912	GAB3	1.412366	TRAV13-1	2.419864	IGHV1-18	2.828459
COL5A1	1.825704	WISP1	1.479082	SEMA4A	1.23427	NLRP3	1.591467	DCN	2.601771	CXCR6	1.984851
RUNX3	1.70867	OSM	1.72772	CALHM6	2.07267	TNFRSF13	1.68669	PRKCQ-	1.16615	PRF1	1.49695

			8		2	C	1	AS1	1		5
KLHL4	1.362927	CREB3L1	1.433286	IGLV5-45	4.512147	EMP3	1.402333	ITGBL1	1.639876	TRAV17	2.021355
TRAV8-6	2.034253	NCF1	1.887392	RRAD	1.316105	GGTA1P	1.204838	ADAMDEC1	2.972679	PLA2G2D	3.225196
EGR2	1.635896	SYTL3	1.497232	IGLV6-57	3.187769	CALB2	1.853488	TNFSF13B	1.723145	PODN	2.310405
IGHV3-35	2.417521	IGHA1	3.170104	ABR	1.1567	KCTD12	1.595486	PLA2R1	1.231173	HEPH	1.600565
TRAV9-2	2.182353	PLB1	1.301387	PLCXD3	1.338223	SMOC2	1.684828	CHI3L2	2.273618	CIITA	1.436349
MCOLN2	1.968809	TRAV29DV5	1.73707	C16orf89	4.865873	TIMD4	2.120265	CD163	1.659101	VSIG1	2.01489
SLIT2	1.944794	IGLV9-49	2.756287	TRAC	2.032218	IL18RAP	1.422285	WDFY4	1.784472	COTL1	1.590796
TRAV5	2.001115	PLAC9	2.017072	GNGT2	1.337858	AL583785.1	1.102424	S1PR4	1.794307	IGHV1-69D	2.812115
DES	3.423965	CYBB	1.970498	GPRC5A	2.14629	SOCS3	1.396103	AC008759.3	1.119974	CCBE1	2.161142
VSIG4	1.814301	FGR	1.387871	ICAM3	1.819236	PLAC8	1.961447	MAMDC2	2.033331	IGFN1	5.265016
TPSB2	2.063269	TRBV12-4	1.964001	AP000892.3	1.447893	LINC01094	1.537324	MPEG1	1.473019	CCND2	1.15734
PNMA2	1.556596	C1QTNF1	1.459716	CD180	1.672882	APOBEC3A	1.456438	IGHV1-67	2.389666	CD70	2.571422
SELL	1.671164	DPEP2	1.35292	LAMA2	1.852132	CFD	1.369742	GNG2	1.23843	TRBC2	1.903715
NRROS	1.212811	LINC01943	1.352693	CD40LG	1.70637	P2RY12	1.957934	TRIM22	1.085356	DUOX2	2.779909
THE	1.61	DOK2	1.52	RAB	1.73	CD30	1.57	GIM	1.14	INSL	1.24

MIS2	7888		5644	33A	8191	0C	2342	AP6	7258	3	4319
FPR3	1.754223	IGHV4-61	2.72033	ELN	1.464577	APOBEC3G	1.35703	IGLV1-44	2.701247	CD3E	2.047897
PROCR	1.08441	LY86	1.570453	TRBV13	2.115926	SIRPB2	1.819617	DGKA	1.114977	SIGLEC14	1.89016
GPRIN3	1.094092	CXCL11	1.421425	TRBV30	1.136939	XCR1	2.560548	TRAV8-3	2.261239	IGHV1-58	4.441232
ZBP1	2.002002	AC109446.3	1.516242	C1QB	1.802936	TMIGD2	1.44566	TRBV11-2	2.109251	WDR86	1.701623
TNFRSF8	1.782644	GCSAM	1.442348	PTGIS	2.241505	IGLV2-11	3.19938	SIGLEC1	1.492172	KLHL6	1.718093
AIF1	1.444826	CDH3	2.209621	IGHV4-34	2.298693	COL1A2	1.970467	FCMR	1.785798	TMEM158	1.851987
SPOCD1	1.329684	AC012645.3	1.484597	EOMES	1.957747	IL16	1.417594	IL24	1.555286	IGHV3-48	2.974119
NFAM1	1.779909	CDX1	1.261148	TRG-AS1	1.617056	EVI2A	1.661546	VILL	1.074436	GFRA2	1.34512
CD84	1.787845	TRAV20	2.489275	CLEC5A	1.562222	CD86	1.607014	CCL18	1.523715	ARL11	1.386886
IGHV3OR16-9	2.989142	TRAV12-2	2.135157	OLFML2B	1.583306	TRAV8-4	2.08648	IGKV2D-40	4.43225	CD52	1.91445
COL16A1	1.613211	AC004847.1	1.652476	TCL1A	2.63752	LINC02084	1.78799	HAMP	1.90044	CELF2	1.853013
CORO1A	1.765059	IGKV5-2	2.690901	LPAR5	1.53376	MAP4K1	1.593592	KLHDC7B	1.373402	AC027031.2	1.702311
SAMD9	1.055685	CRISPLD1	1.532572	LTF	1.483106	AC011899.2	1.281964	IGKV3-15	3.083251	EPHA3	2.137343
CXCL9	2.215335	FMN1	1.277511	ADGRE1	2.135018	POSTN	2.082384	CSF2RB	1.775343	IGKV6-21	4.431687

SPTSSB	1.5624	IGHV6-1	2.948047	AL078590.3	1.122331	IGLV2-18	1.963697	MGP	1.751877	NLRC3	1.411631
LSAMP	1.27995	CLEC10A	1.32439	FAP	2.179696	TRBV24-1	2.269855	IGKV3-20	2.507304	GPR34	1.275499
CTSK	3.050439	NCKAP1L	1.755665	PAMR1	1.785939	KLHL30	1.481979	PRELP	2.374445	P2RY13	1.755454
TRBV5-4	2.085543	IL10	1.975458	EVI2B	1.801425	CMTM2	1.197374	RYR1	1.556865	IGKV3-7	2.995016
IGHV2-70D	3.276647	AL034397.3	1.553627	EGR3	1.523698	TMEM200A	1.698375	IGKV1-12	2.879063	MYL9	2.07684
LINC01150	1.380106	IKZF1	1.884509	SIGLEC8	1.966858	PSTPIP1	1.58811	ICAM1	1.062879	AC015911.3	1.765126
IGHV3OR16-13	2.828041	LXN	1.630104	VENTX	1.098231	SRPX	2.894151	AC004687.1	1.587409	TRBV7-6	2.102254
IGHV3-19	3.277471	TRBV10-3	2.019024	HLA-DOA	2.003897	ARHGDIB	1.246424	SLC7A7	1.300381	LINC00892	1.501468
TMPRSS4	2.912905	IGHV1-3	2.797201	COL1A1	2.007241	CCR1	1.541218	PTPRC	1.977651	IPCEF1	1.564924
FDCSP	1.350445	MMP7	2.339242	GSTM5	1.381357	NCF1C	1.603543	JCHAIN	2.763558	IGKV2D-24	2.851759
FASLG	1.821436	RTN1	1.193506	ADA2	1.198986	P2RX1	1.712914	LILRA1	1.356257	IGHGP	2.985436
ANK2	1.547976	IGKV1-16	2.556565	HLA-DQB1	1.792383	AC015911.7	1.726598	LINC01615	1.988205	LILRB5	1.214507
CLMP	1.78213	SIRPG	1.838397	CEACAM6	2.699604	LAIR1	1.543155	RNU4-62P	1.428506	LILRA5	1.58151
SFRP1	2.404552	IGKV3OR2-268	1.964073	LINC02285	1.355245	AC245128.3	1.702526	AC004585.1	2.09028	IGHV3-72	3.042385
ARH	1.54	GZM	1.79	AC0	1.37	IGHV	1.80	PLD4	1.49	PTGS	1.89

GAP30	7029	A	983	08105.3	0859	7-81	5645		7204	2	0138
TRDV1	2.609861	C11orf21	1.531822	IGKC	2.836288	PRRX1	1.626222	C3AR1	1.512788	CRPP1	1.307358
C1QC	1.695954	TRBV18	1.994116	HAND2	2.76267	LINC01857	2.177317	POU2AF1	1.780768	SPIB	1.739411
TRBV5-1	2.132398	CD27	2.194958	FCGR2A	1.333484	IGHV3-15	3.405438	GPR68	1.75152	TLR2	1.147651
IL10RA	1.555517	DACT1	1.278637	LTBP2	1.647119	IGHG2	3.214813	CD300A	1.427742	CD177	3.011076
FCER2	2.0211	GIMAP7	1.0914	HLA-DMB	1.674165	ASB2	1.783387	SYK	1.41717	SEMA4D	1.234038
GLI3	1.528462	FGF7	2.499792	WISP2	2.805275	INTS6L	1.154337	AC015819.1	1.307339	GVINP1	1.626248
IGKV2D-29	2.618559	AC090559.1	1.540693	TAGAP	1.899712	IGHV3-33	3.349049	SIT1	1.978719	PRAM1	1.354916
ADAM33	1.837252	IGHV3-63	1.481165	AL031846.1	1.472813	TLR7	1.915069	LINC01480	1.580077	MGAT3	1.395534
FSTL3	1.107366	GAL3ST4	1.825669	SIDT1	1.228792	IGLV2-8	3.714585	SPOCK2	1.343944	C14orf180	1.415586
LRRC17	1.267248	PTN	1.935031	CD48	1.968469	NDRG4	1.770442	TRBV6-1	1.913145	TWIST1	2.202654
INPP4B	1.351267	CHIT1	3.764407	GPR65	1.751135	TMEM173	1.547338	SLAMF7	2.255376	IL1B	1.517349
AC142381.1	3.023204	GREM1	1.363277	STRA6	1.602313	IGLV8-61	3.440634	SYNDIG1	1.577552	IGHV1-2	3.724027
POU2F2	1.593397	COL6A1	1.313795	GNA15	1.436492	GFPT2	2.002753	HAVCR2	1.562833	ARHGAP25	1.271364
CXCR1	1.581905	GLIPR1	1.241136	FTH1P22	2.018011	LINC01679	1.507177	HSPB2	1.846561	CCR5	2.038009

CD3G	1.923848	IGHJ3	3.017445	ZBED2	2.226592	PTHLH	1.280356	IGLV3-25	2.772691	SPN	1.78941
LY9	1.955246	PRUNE2	1.807226	GPR174	2.33319	IGHG3	2.592775	CST7	1.731666	AIM2	2.575125
SGCA	2.016889	IGLV1-51	2.731758	AC025031.1	1.154675	PLA2G4A	1.483604	FAM129A	1.538228	ADGRE2	1.771439
TRPV6	1.371094	RAB31	1.366481	TRBV3-1	2.377896	CD72	1.621471	IL6	1.47589	LAX1	1.726707
BIN2	1.591724	ALOX5AP	1.841305	SNX20	1.857561	CLEC4E	1.99277	CD8A	2.134361	IGKV2-29	1.93397
AL135818.1	1.512786	ARHGAP9	1.65561	FBN1	1.49824	GPR171	1.958754	TRAV2	2.144153	FOXF1	1.616016
EMILIN2	1.197636	S100B	1.134815	GPX8	1.293373	HNRNPA1P21	1.706362	TMSB4X	1.048943	IGLV1-50	1.843165
SLFN12L	1.774613	IGKV1-5	2.894504	COL3A1	2.159941	IGHV1-12	2.764672	HCK	1.688893	ADAM12	1.269018
CRTAC1	5.532685	PMP22	1.461252	XYLT1	1.494491	MMP9	1.340616	MSR1	1.416241	ISLR	2.841873
CSF2RA	1.111801	GPNMB	2.207298	ITGA3	1.426091	HAPLN3	1.872194	PIK3R5	1.564589	GNB4	1.224823
LTA	1.847	PRDM1	1.378307	IGLV3-21	3.090114	OSCAR	1.427126	CD80	1.833318	SIGLEC11	1.352497
FCRL6	1.354542	RASGRP1	1.808062	IGHV1-24	3.275489	CD300LF	1.528796	CLEC1B	3.096037	IGLV1-40	3.189485
MUC1	1.831454	CD22	1.673789	MEI1	1.669101	HAS1	2.458546	ADTRP	1.376373	TESPA1	2.033476
TRAV14DV4	2.102753	LYPD5	1.238588	IGLC6	2.383551	CR1	2.364655	CD38	1.770606	AC100803.2	1.655392
CPA3	1.44734	PI16	2.42225	SIRPB1	1.75785	COL8A2	1.70916	IGHV5-51	2.76703	MIAT	2.30037

	7		3		5		6		9		1
HCLS1	1.60809	CHST2	1.41724	ACKR1	2.277061	IRAK3	1.255004	INMT	2.080167	AL590483.2	-1.88135
TM6SF1	1.514893	ABI3BP	1.665924	BHLHE22	1.883783	SCGB3A1	1.087448	FYB1	1.921132	ABHD1	-1.48554
FAM167A	1.304946	SIGLEC9	1.624366	DSE	1.352911	AP002954.1	1.656441	CAMKK1	1.174461	CTNNA2	-1.71756
HS3ST2	1.449375	CD1B	2.121584	STAB1	1.167569	TSHZ3	1.486788	PLEKHO2	1.100244	GREB1	-1.31633
BLK	1.496161	AC145098.1	1.188015	PILRA	1.290937	IKZF3	1.830501	THBS2	2.181602	AC104088.1	-1.75
IGHV3-38	2.307089	GPSM3	1.478327	IGKV3-11	2.93285	CD2	2.017927	CCR7	2.252418	AC098934.2	-1.19748
HTRA3	1.557983	IGHM	2.839508	HBD	2.294156	PYGM	1.522747	C6orf222	1.419727	AC010501.1	-1.33218
RGS18	1.543877	GGT5	1.905747	IGFBP6	1.553106	BTK	1.691727	CLEC4A	1.162197	AC114947.1	-1.33123
CAMK4	1.584642	JAKMIP1	1.762361	C11orf96	1.460009	MAP1A	1.975332	EPB41L3	1.636321	AC231981.1	-1.13135
RAC2	1.547646	TNXB	1.790849	AC015911.8	1.976381	LINC01871	1.633906	FOXS1	1.398251	LGR5	-1.55644
CLEC7A	1.778485	CRISPLD2	1.908089	NCF1B	1.790094	TRAV16	2.023215	AL161935.3	1.235889	PAGE4	-1.77836
GPR84	2.149954	GNG8	1.446281	IGHV4-59	2.270145	WDR86-AS1	1.265675	LILRB4	1.874236	AOX3P	-1.14283
TOMM20P2	1.51614	PDE6G	1.333988	TRBV4-2	2.064223	CXCL12	1.459046	NMUR1	1.290986	KCNU1	-1.69174
GZMM	1.378178	SCIMP	1.675269	DUOXA2	2.337249	EMB	1.925078	TNFSF18	1.133181	RHBDL3	-2.18423
CD79	2.71	PI3	2.08	CR2	3.71	LINC	1.28	1-Mar	1.24	RAS	-

A	4354		6922		9856	00426	3269		3829	L10B	1.79163
CLEC2B	1.332659	ANTXR1	1.795688	CYSLTR1	1.298175	LINC01133	2.693966	TMC8	1.589352	DNAJB3	-1.39467
DOCK8	1.183959	TRAV19	2.26379	TRBV28	1.989384	SVEP1	2.26877	MYEOV	2.971353	LINC01970	-1.48494
TBX21	1.461332	FGD2	1.41106	GPM6A	1.775044	PCDH7	2.089058	TLR10	1.726541	AC011747.1	-1.58552
SASH3	1.816257	CRTAM	2.142564	IGHV3-21	2.795131	IL2RB	1.791157	TYROBP	1.416242	AC026765.2	-1.68538
CD1C	1.455149	LILRA4	1.693925	CYTIP	1.693154	IGKV1D-43	2.638579	TRBV2	2.111122	RNF43	-1.15277
CLEC12A	1.837451	FAM163B	2.156003	MT1L	1.143375	IL18BP	1.33826	NCR1	1.511197	IQCH	-1.17561
IGKV1D-42	4.825363	MRC2	1.810258	NDNF	3.203979	IGLV10-54	4.44073	CHRNA1	3.747691	AC008549.1	-1.30317
CCR2	1.624944	C1orf162	1.490718	CEACAM4	1.627638	CD5	2.040592	IGHV4-55	2.658869	RNU6-46P	-1.23746
SAA1	1.680038	IL1RL1	1.825935	HCG11	1.404766	CXCL3	1.427826	IDO1	1.270372	MIR325HG	-1.40529
WNT10A	1.8459	GPBAR1	1.901086	PLAU	1.864251	MILR1	1.41197	CD19	1.720654	SP5	-1.35922
CD33	1.480636	LINC00996	1.493434	LUM	2.746703	MS4A4E	1.216535	RASGRP4	1.227814	LINC02587	-2.14413
FGD3	1.114504	FCGR3A	1.529517	CD37	1.708955	CCL19	3.858908	GDF6	1.546423	PHYHIPL	-1.13104
IGHV3-73	3.931512	AC134043.2	1.319689	IFI44L	1.290179	NGFR	1.870336	SAMD9L	1.413463	ACTN2	-1.72635
TSPAN32	1.291535	MMP19	1.003688	DOCK2	1.812872	SAMSN1	1.813943	PTCH2	1.484237	AC007277.1	-1.89145

FAM78A	1.298779	TRBJ2-1	1.895605	SPI1	1.523288	ZG16B	1.245546	IGHV2-5	2.843498	AC010531.5	-1.19432
FCN3	1.952668	AC243960.1	1.688985	MAL	2.215366	TRAF3IP3	1.719393	AL365361.1	1.975952	ACSL6	-1.40132
CXCL5	1.787976	THEMIS	2.110969	CD247	1.569931	IL12RB1	1.696024	ITGB6	1.972406	AC113404.1	-1.32862
PTGER3	1.492873	TRBV29-1	2.311921	PLEKHS1	2.013227	FCGR1A	2.045095	IGHV2-26	3.264057	AC069294.1	-1.54166
KCNN4	2.213259	TRGV7	1.613288	BCL11B	1.696699	AP005019.1	1.728298	IGHV3-11	3.574893	LINC01124	-1.34115
TRAV12-1	2.297568	HLA-DQB1-AS1	1.640868	TLR8	2.268874	TRBC1	2.030253	MT1F	1.019457	AL163953.1	-1.50539
SHISA3	2.639044	IFI16	1.167215	GPR182	1.854023	IL2RG	1.707784	CDH17	1.842655	C5orf66	-1.25871
BANK1	2.399321	RUBCNL	1.600165	WNT2	3.288091	AC002398.2	2.175323	ZAP70	1.555357	NOTUM	-1.55725
AC110995.1	1.263349	PTAFR	1.376067	AC115522.1	1.443892	TREM2	1.282343	MIR8071-2	2.504692	HLF	-1.13434
GATA3	1.413084	CLEC11A	1.776843	LYL1	1.141136	HLA-DRA	1.679208	CLEC9A	1.706703	TECTB	-1.21056
AC022730.4	1.270713	TRBJ2-7	1.930686	LINC02544	2.052544	CCL11	2.326153	HLA-DRB6	1.626719	AC013244.1	-1.26814
CHN1	1.205783	DNM3OS	1.592814	RASSF2	1.640809	CFP	1.617471	DNAJC5B	1.772272	AC007406.2	-1.28226
FCGR1CP	2.011366	EFEMP1	1.881219	MYO1G	1.517333	PYHIN1	1.842306	IGHV3-23	3.109137	ASB4	-1.25158
SOD3	1.842559	HVCN1	1.187349	HLA-DPB2	1.739027	SFMBT2	1.083718	IGKV1-9	3.361738	GALR3	-1.12335
AEBP	2.47	SUSD	2.56	CHR	2.03	TME	1.42	TRB	2.22	AL02	-

1	3909	5	6649	DL1	4152	M71	2634	V6-6	4608	3583.1	1.12478
PTGER2	1.363274	SFTA2	2.488833	MS4A6A	1.659303	FOSB	1.379381	MRVI1	1.615506	SRARP	-1.25968
DUSP4	1.351007	FABP3	2.01285	GLT8D2	1.664265	PTPN7	1.760733	LINC02446	2.281266	C1QTNF3	-1.86
F3	1.275467	IGSF21	1.155595	COL6A2	1.638485	KLRD1	1.356252	SSC5D	1.97987	PLPPR1	-1.14827
MNDA	1.67742	IGHV1OR15-2	2.986932	ZNF683	1.877092	TRAV3	2.131101	CILP	1.90536	GLULP4	-1.40981
NMNAT2	2.430594	TIGIT	2.068184	CPXM2	1.910928	TSPAN11	1.231899	AC079015.1	1.295176	AP000593.3	-2.02394
AC013264.1	1.921101	KEL	2.238381	CLECL1	1.707293	STMN2	2.640364	PCBP3	1.433234	GLUL	-1.445
MOXD1	2.589764	IGHV3-71	3.444001	FMNL1	1.25064	OGN	2.386333	IGHV2-70	3.312159	LINC00886	-1.11682
IGLV3-16	3.791072	TRBV6-5	1.836209	STAB2	1.940494	PLTP	1.572118	CXCL14	2.30272	HIST1H4PS1	-1.19896
PLXDC1	1.367727	SCARA5	3.019923	CADM3	2.239388	TRBV5-6	2.523338	ITK	1.999011	AC090150.1	-1.15498
LILRB1	1.762417	HLA-DQA1	1.953079	CD226	1.757418	CD5L	1.783225	CCL4	1.620681	AC007406.1	-1.07039
WAS	1.284839	CYTH4	1.362738	HLA-DPB1	1.68485	CTSG	1.552515	IGHV1OR15-9	2.479737	FAM169A	-1.21733
TFEC	1.859993	FCGR1B	1.812278	TRAV4	2.159244	ADGRB2	1.658967	LOXL1	2.72725	AC005841.1	-1.22751
AF127936.1	1.566555	TRBV27	2.133081	C2CD4A	1.089338	TRAV23DV6	2.397153	TNNT3	3.507232	RGSL1	-2.20544
ARHGAP1	1.58464	GALNT5	3.10131	TRDC	1.66586	IGKV1OR2-	2.09302	IGLV2-14	2.49321	AP001331.	-1.89

5	3		7		8	108			5	1	468
NCF4	1.418468	HLA-DQA2	1.812434	IGKV1-6	2.575147	TACSTD2	1.572414	ADAMTS15	1.639236	MTND4LP30	-1.31629
AL590648.3	1.431309	P2RY10	1.771844	MMP12	2.402226	CERKL	1.382172	FERMT3	1.526647	TBX3	-1.24349
TRGV10	1.642772	CLIC6	1.45859	ANXA1	1.432917	AC026369.3	1.810872	SIGLEC10	1.850716	RHBG	-1.78067
AC006059.1	1.297365	SIGLEC12	1.313513	NCR3	1.64258	IGHV3-41	1.908937	GABRP	2.604731	KLK4	-2.89054

DEGS, differentially expressed genes.

Supplementary Table S3 PPI network core genes from DEGs screened by ImmuneScore and StromalScore

Gene	Count	Gene	Count	Gene	Count	Gene	Count	Gene	Count	Gene	Count
CXCL8	25	CD86	8	ALOX5	3	MMP7	2	CFP	1	LCP1	1
SYK	25	HCK	8	ANXA1	3	NLRP3	2	CHN1	1	LGALS9	1
CXCL12	22	HLA-DMB	8	C1QA	3	NTF3	2	CLEC4E	1	LGR5	1
CCL5	20	HLA-DQA2	8	C1QB	3	NTRK2	2	CLEC7A	1	LOXL1	1
CXCL1	20	IL6	8	C3AR1	3	P2RY10	2	COL16A1	1	LTF	1
CD4	19	ITK	8	CCR4	3	PLCB2	2	COLEC10	1	LY86	1
LCK	19	CD79A	7	CD33	3	PTGIS	2	COTL1	1	LYVE1	1
CXCL11	18	COL5A1	7	CD72	3	RHOH	2	CR2	1	MAP4K1	1
CCL4	16	COL6A1	7	CLEC1B	3	RIPK3	2	CSF2RA	1	MMP12	1
CXCL9	16	HLA-DQB2	7	CLEC5A	3	S1PR4	2	CTSG	1	NCKAP1L	1
IL10	16	HLA-DRB5	7	CSF1R	3	SAA1	2	DOCK2	1	OGN	1
LCP2	16	IL2RG	7	CXCR6	3	SELP	2	DOK2	1	OMD	1
CD3E	15	CD19	6	GNG2	3	SEMA4	2	DUO	1	OMG	1

						D		X2			
CXCL5	15	CD8A	6	ITGA3	3	SH2D1A	2	DUOXA2	1	PDE6G	1
CXCR4	15	COL6A2	6	ITGA4	3	SLA	2	EFNB3	1	PDPN	1
CCL19	14	COL6A3	6	ITGB6	3	SOCS3	2	EGR2	1	PIK3R5	1
CCL21	14	DCN	6	LUM	3	SPI1	2	EGR3	1	PLAU	1
CCR5	14	FCGR3A	6	MMP2	3	TBX21	2	ELN	1	PLN	1
VAV1	14	FPR1	6	NCF1	3	TBXAS1	2	EPHA3	1	PRF1	1
CCR2	13	IL1B	6	NCF4	3	TNFRSF13C	2	EVI2A	1	PTCH2	1
HLA-DRA	13	ITGAX	6	NGFR	3	TREM2	2	EVI2B	1	RNF43	1
ZAP70	13	WAS	6	PRKCQ	3	VSIG4	2	FCGR1B	1	RUNX3	1
CCR1	12	CCL11	5	SELPLG	3	WIPF1	2	FCN3	1	SELL	1
ITGB2	12	CD80	5	TNFSF13B	3	ABI3	1	FLT3	1	SIGLEC14	1
PTPRC	12	CYBB	5	VCAN	3	ABI3BP	1	FPR3	1	SIRPB1	1
BTK	11	GNB4	5	ARHGDIB	2	ACKR1	1	GATA3	1	SLA2	1
CD247	11	PTGS2	5	C1QC	2	ACTN2	1	GBP5	1	SLAMF1	1
COL1A1	11	PTPN22	5	C5AR1	2	ADAM28	1	GLI3	1	SLAMF6	1
CXCR2	11	ADAMTS2	4	CCL22	2	AIM2	1	GPR84	1	SOD3	1
CXCR3	11	CD2	4	CD300A	2	ALOX5AP	1	GPSM3	1	STAB2	1
HLA-DRB1	11	CD22	4	CD40LG	2	ANK2	1	GPX8	1	TCN1	1
TYROBP	11	CD53	4	CD5	2	ARHGAP9	1	GZMA	1	TLR2	1
CD74	10	CIITA	4	CLEC12A	2	ATP2A3	1	HAVCR2	1	TLR7	1
CXCR1	10	CSF2RB	4	DAPP1	2	BIN2	1	HCLS1	1	TLR8	1
HLA-	10	FCGR	4	FBN1	2	BIRC3	1	HLA-	1	TME	1

DQA1		1A						DOA		M173	
RAC2	10	FGR	4	FCGR2A	2	BLK	1	IFI16	1	TNFRSF17	1
CCR7	9	GNA15	4	FZD2	2	C7	1	IL10RA	1	TNFRSF8	1
COL1A2	9	GNGT2	4	GNG8	2	CAMK4	1	IL16	1	TNFSF8	1
COL3A1	9	HLA-DPB1	4	ICAM3	2	CAMKK1	1	IL18BP	1	TNNT3	1
CXCL3	9	ICAM1	4	IL21R	2	CD177	1	IL18RAP	1	TRIM22	1
HLA-DPA1	9	IL2RA	4	IL7R	2	CD180	1	IL34	1	WNT10A	1
HLA-DQB1	9	LILRB2	4	INPP5D	2	CD209	1	ITGA9	1	WNT2	1
IL2RB	9	MMP9	4	LAIR1	2	CD27	1	KLRD1	1	ZBP1	1
JAK3	9	PLAUR	4	LPAR1	2	CD300E	1	L1CAM	1		
CD3G	8	TIMP1	4	LPAR5	2	CD70	1	LAMA2	1		

Supplementary Table S4 Poor prognosis related genes from DEGs screened by ImmuneScore and StromalScore

gene	KM	HR	HR.95L	HR.95H	*p*value
PTPRO	0.033424	2.238024	1.152786	4.344911	0.017312
SPOCD1	0.015313	1.213828	1.035583	1.422752	0.016781
SPTSSB	0.046119	1.068222	1.011319	1.128328	0.01813
HTRA3	0.011235	1.043528	1.011301	1.076781	0.007765
GPR84	0.031833	1.27537	1.104376	1.472839	0.000927
CXCL5	0.023003	1.009484	1.002221	1.016799	0.010397
PLAUR	0.021906	1.023605	1.003917	1.043679	0.018546
TRBV10-3	0.04285	0.267878	0.11143	0.643977	0.003247
CLEC5A	0.00539	1.780853	1.233664	2.570747	0.002062
STRA6	0.012942	1.297887	1.036369	1.625397	0.023139
KLRB1	0.04135	0.866394	0.785469	0.955656	0.00415
IL7R	0.006566	0.892265	0.800464	0.994594	0.039607
IL18RAP	0.001203	0.302831	0.131081	0.699614	0.005172
LINC01094	0.043624	2.006601	1.392642	2.891228	0.000186
MMP9	0.009448	1.003832	1.000028	1.007651	0.04833
LINC00426	0.003218	0.186921	0.037245	0.938083	0.041588
TREM2	0.021588	1.018437	1.003249	1.033854	0.017166
FLT3	0.048108	0.151001	0.030576	0.745719	0.020339

MSR1	0.040151	1.12339	1.026461	1.229472	0.011496
ITGB6	0.002084	1.293882	1.046206	1.600191	0.017471

HR, Hazard Ratio.

Supplementary Table S5 Antibodies used in this study

Name	Supplier	Cat no.
FITC anti-mouse CD11b antibody	BD	#557396
PE anti-mouse Ly-6G/Ly-6C antibody	BD	#553128
PE-CF594 anti-mouse CD11c antibody	BD	#562454
PERCP anti-mouse CD3 antibody	BD	#551163
PE-CY7 anti-mouse CD86 antibody	BD	#560582
APC anti-mouse CD206 antibody	BD	#565250
AF700 Fixable Viability Stain	BD	#564997
APC-CY7 anti-mouse CD45 antibody	BD	#557659
BV421 anti-mouse F4/80 antibody	BD	#565411
BV480 anti-mouse IA/IE antibody	BD	#566086
BV605 anti-mouse CD19 antibody	BD	#563148
BV650 anti-mouse NK1.1 antibody	BD	#564143
FITC anti-mouse CD8a antibody	BD	#553030
PE anti-mouse CD152(CTLA-4) antibody	BD	#553720
PE-CY7 anti-mouse CD44 antibody	BD	#560569
APC anti-mouse CD62L antibody	BD	#553152
BV421 anti-mouse CD4 antibody	BD	#562891
BV510 anti-mouse CD223(LAG3) antibody	BD	#746508
BV605 anti-mouse CD279(PD-1) antibody	BD	#563059
BV650 anti-mouse CD366(TIM-3) antibody	BD	#747623
PE anti-mouse GranzymeB antibody	BD	#12-8898-82
APC anti-mouse IFNγ antibody	BD	#554413
Ms CD16/CD32 Pure 2.4G2 100ug	BD	#553141
BB515 anti-human CD4 antibody	BD	#564419
PE anti-human CD47 antibody	BD	#556046
BB700 anti-human CD8 antibody	BD	#566452
Alexa Fluor647 anti-human GranzymeB antibody	BD	#560212
APC-CY7 anti-human CD45 antibody	BD	#557833
BV421 anti-human CD56 antibody	BD	#562751
BV510 anti-human CD19 antibody	BD	#562947
BV605 anti-human CD3 antibody	BD	#562994
BV786 anti-human IFNγ antibody	BD	#563731
BV421 anti-human CD183(CXCR3) antibody	BD	#562558
MMP9 (N-terminal) Polyclonal antibody	Proteintech	#10375-2-AP
MMP9 antibody	BOSTER	#PB9669
SSH1 Polyclonal antibody	ECM	#SP1711
CXCR3 Polyclonal antibody	Proteintech	#26756-1-AP

CXCR3B-specific Monoclonal antibody	Proteintech	#60065-1-Ig
SIRT2 Monoclonal antibody	Proteintech	#66410-1-Ig
ERK1/2 Polyclonal antibody	Proteintech	#11257-1-D8
Phospho-ERK1/2 (Thr202/Tyr204) Polyclonal antibody	Proteintech	#28733-1-AP
Phospho-Akt (Ser473) Rabbit mAb	CST	#4060
Akt (pan) Mouse mAb	CST	#2920
JMJD2D Antibody (F-7)	Santa Cruz	#sc-393750
Granzyme B Rabbit pAb	Abclonal	#A2557
KDM4D Rabbit pAb	Abclonal	#A18138
GAPDH antibody	Proteintech	#15143-1-AP
CD8	Abcam	#ab209775
IFN	Affinity	#DF6045
β-catenin	PTG	#51067-2-AP
Flag antibody	Sigma	#F1804
HA antibody	Sigma	#SAB4300603
MYC antibody	Santa Cruz	#sc-40X
IgG(mouse)	Santa Cruz	#sc-69786
IgG(rabbit)	CST	#3900

Supplementary Table S6 Primers and shRNA used in this study

Primiers	Sequences
homo-MMP9-F	TGTACCGCTATGGTTACACTCG
homo-MMP9-R	GGCAGGGACAGTTGCTTCT
mus-MMP9-F-1	GCAGAGGCATACTTGTACCG
mus-MMP9-R-1	TGATGTTATGATGGTCCCACTTG
mus-MMP9-F-2	CTGGACAGCCAGACACTAAAG
mus-MMP9-R-2	CTCGCGGCAAGTCTTCAGAG
mus-CD44-F	TCGATTTGAATGTAACCTGCCG
mus-CD44-R	CAGTCCGGGAGATACTGTAGC
mus-MYC-F	ATGCCCCTCAACGTGAACTTC
mus-MYC-R	GTCGCAGATGAAATAGGGCTG
mus-CyclinD1-F	GCGTACCCTGACACCAATCTC
mus-CyclinD1-R	ACTTGAAGTAAGATACGGAGGGC
homo-GAPDH-F	CTGGGCTACACTGAGCACC
homo-GAPDH-R	AAGTGGTCGTTGAGGGCAATG
mus-GAPDH-F	AGGTCGGTGTGAACGGATTTG
mus-GAPDH-R	TGTAGACCATGTAGTTGAGGTCA
shRNA target	Sequences
mus-MMP9-sh	CAGTACCAAGACAAAGCCTAT
mus-KDM4D-sh1#	CCACGGTAAGTAACGTTCCTT

mus-KDM4D-sh2#	ACACAGAGACTATGGTGTCTA
mus-SSH1-sh1#	CCCGTTTAGATCACACCAGTA
mus-SSH1-sh2#	GCAGCGATGAAGAACGGAAAT